

A Semiclassical Approach to Relativistic Nuclear Mean Field Theory

M. CENTELLES, X. VIÑAS, AND M. BARRANCO

*Departament ECM, Facultat de Física, Universitat de Barcelona,
Diagonal 647, E-08028 Barcelona, Spain*

AND

P. SCHUCK

Institut des Sciences Nucléaires, 53 Avenue des Martyrs, F-38026 Grenoble-Cédex, France

Received February 27, 1992; revised June 10, 1992

Semiclassical relativistic particle and energy densities for a set of fermions submitted to a scalar field and to the time-like component of a four-vector field are derived in the Wigner–Kirkwood and Thomas–Fermi mean field theories, including gradient corrections up to order \hbar^2 . As a test of the validity of the semiclassical method, a simple case is studied, where the scalar potential and the zero component of the four-vector potential are identical and correspond to a harmonic oscillator. The semiclassical approach is then applied to the non-linear $\sigma - \omega$ model and the resulting variational equations are solved for finite nuclei and semi-infinite symmetric nuclear matter. In this case Hartree solutions are available and allow for an additional test of the reliability of the \hbar^2 corrections. © 1993 Academic Press, Inc.

1. INTRODUCTION

The description of nuclear properties by means of relativistic mean field theories has been a subject of growing interest during recent years. One of the most popular models is the relativistic quantum field theory for the nuclear many-body problem developed by Walecka and co-workers [1, 2] (for a review, see Refs. [2, 3]), originally conceived to describe the behaviour of the nuclear equation of state. This approach contains both nucleonic and mesonic degrees of freedom and can be considered as phenomenological. The coupling constants and some meson masses of the effective meson–nucleon Lagrangian are taken as free parameters which are adjusted to fit the properties of nuclear matter and finite nuclei. Most calculations have been carried out in the mean field Hartree approximation, in which exchange terms are neglected and the contributions from antiparticles are not included [4–6].

In the standard model of Walecka the incompressibility of nuclear matter is overestimated. The inclusion by Boguta and Bodmer [7] of non-linear contributions

through cubic and quartic terms in the scalar field, shifted the incompressibility to more reasonable values in comparison with empirical data. The non-linear $\sigma - \omega$ model has been widely used in recent applications (see, e.g., [5, 6, 8–10]), as it yields a successful description of the ground-state properties of finite nuclei. More fundamental approaches have also been investigated in the relativistic framework, as is the case of Dirac–Hartree–Fock [11, 12] or Dirac–Brueckner–Hartree–Fock [13–15] methods.

However, most of these applications are, as in the case of their non-relativistic counterpart, quite complicated on a purely quantum mechanical level. In non-relativistic nuclear physics, semiclassical models have become very popular [16–18] due to their reliability and feasibility, as they avoid the task of solving the quantal mean field Hartree–Fock (HF) equations. These models have been mainly used together with effective density-dependent nuclear interactions, such as the Skyrme or Gogny forces.

Usually, semiclassical methods are based on the Wigner–Kirkwood (WK) \hbar expansion of the density matrix [19]. In the extended Thomas–Fermi (ETF) method the total energy of a nucleus is expressed as a functional of the local particle density and its gradients (see [20, 21] and references quoted therein). The ground-state density distribution is found from the energy density functional by a variational approach. The theoretical justification of this so-called energy density formalism [22] is given by the Hohenberg–Kohn theorem [23]. To cure the deficiencies of the lowest-order Thomas–Fermi (TF) approximation and thus provide a more accurate description of the nuclear surface, at least \hbar^2 -order gradient corrections coming from inhomogeneity and non-local effects have to be included in the energy density functional. The ETF method smoothes out quantal effects and one is left with the average part of the HF energy and thus can be considered similar in spirit to the droplet model [24]. The remaining part of the energy, which is much smaller, is of a purely quantal origin and can be added perturbatively to the semiclassical smooth quantity, as indicated by the Strutinsky energy theorem [25]. Detailed ETF calculations compared with the corresponding HF ones can be found in Refs. [21, 26].

The basic theorem of Hohenberg and Kohn was extended to the relativistic domain (see, e.g., [27]), thus laying the foundations of relativistic density functional theory. Relativistic \hbar corrections to the TF approximation have been introduced in the atomic context on the basis of a field theoretical formulation by Dreizler and collaborators. In the derivation of such corrections these authors first used the gradient expansion method of Kirzhnits [28] (Gross and Dreizler in [17, p. 81]; [29, 30]), and later an alternative approach based on Green's function techniques [31–33]. Until very recently, semiclassical methods applied to relativistic nuclear physics were not so well developed. For instance, the $\sigma - \omega$ model had only been solved in the simplest TF approximation for finite nuclei [2, 34–36] and for semi-infinite nuclear matter [7, 37, 38]. In comparison with the atomic case, the derivation of \hbar corrections in the nuclear problem has the additional difficulty of the existence of a position-dependent effective mass, originating

from the scalar potential, which makes the semiclassical treatment and expressions more complicated.

In a preliminary paper [39] we have presented the semiclassical relativistic expressions of the particle and energy densities, including \hbar^2 -order gradient corrections, for a set of fermions moving in the mean field arising from a scalar potential and from the time-like component of a four-vector potential. In the derivation of these corrections, a method similar to that employed by Taruishi and Schuck to obtain a semiclassical BCS theory [40] has been used. As an application of the relativistic extended Thomas–Fermi (RETF) method, calculations of finite nuclei within non-linear $\sigma - \omega$ models have been carried out in Ref. [41]. In Ref. [42] the structure of finite nuclei, the fission of rotating nuclei, and the complex optical potential for heavy ion scattering have been studied, using the relativistic kinetic energy density functional of order \hbar^2 , together with a potential energy density obtained from a local density approximation to Dirac–Brueckner calculations.

In this paper a method based on the Wigner transform of operators is presented which provides a transparent and straightforward \hbar expansion of the propagator, valid for time-independent single-particle Hamiltonians with a matrix structure. Our main concern is the application of the method to a scalar-vector Dirac Hamiltonian of interest in relativistic nuclear physics. It is shown how the semiclassical WK and RETF expansions up to order \hbar^2 of ground-state averages of physical quantities are derived from the propagator in the mean field approximation. The semiclassical picture would be somehow incomplete if the study were only confined to formal aspects of the theory, without exploring its versatility in actual applications. To this end, the solutions of the variational equations corresponding to the \hbar^2 expansion are studied for two problems; namely a relativistic harmonic oscillator and the non-linear $\sigma - \omega$ model.

Effort has also been devoted by other authors to the development of semiclassical expansions in the relativistic nuclear framework. Weigel, Haddad, and Weber [43] have used the Green's function scheme and the Wigner representation to obtain \hbar^2 -order WK expressions for a Lagrangian of one-boson-exchange potential structure in the HF approximation. A derivation of the semiclassical approximation to the relativistic finite temperature HF method has been given by Von-Eiff and Weigel [44]. On completion of this work, we became aware of the recent study on the density functional approach to quantum hadrodynamics (QHD) carried out by Speicher, Dreizler, and Engel [45]. These authors have shown the validity of the Hohenberg–Kohn theorem in QHD. On the basis of the Green's function expansion techniques of Ref. [31], the semiclassical non-interacting kinetic energy density is derived to order \hbar^2 , taking into account vacuum contributions and the four components of the vector potential. The specific case of the $\sigma - \omega$ model in the Hartree approximation is also considered, and the corresponding variational equations are derived. However, no numerical applications have been carried out in these studies.

The paper is organized as follows. Section 2 presents the semiclassical relativistic expansion, generalizing the results given in [39] (unfortunately this reference contains some misprints, although the numerical results are correct). In Section 3 the

expressions corresponding to the semiclassical particle and energy densities are discussed. In Section 4 the semiclassical scheme is applied to the case of a relativistic harmonic oscillator where the scalar potential and the zero component of the vector potential are identical. As this problem admits an analytical solution of the Dirac equation, it is an excellent example to test the accuracy of the semiclassical WK and energy density (RETF) approaches, in comparison with the Strutinsky averaging procedure and the quantal results. Section 5 gives results obtained for the $\sigma - \omega$ model using the \hbar^2 corrections. This section complements the calculations recently published for finite nuclei [41] in two ways. First, other parameterizations of the Walecka Lagrangian are used here and the numerical method for solving the \hbar^2 -order variational equations is outlined. Second, an account of the surface properties (density profiles and surface and curvature energies) obtained from the RETF model is given. The last section of the paper presents a short summary. Finally, the appendices provide the expression of the semiclassical density matrix to order \hbar^2 as well as some technical details.

2. \hbar EXPANSION OF THE PROPAGATOR FOR HAMILTONIANS WITH A MATRIX STRUCTURE

In quantum mechanics the problem described by a time-independent single-particle Hamiltonian \hat{H} has an associated propagator defined by

$$\hat{G}(\eta) = \exp(-\eta\hat{H}). \quad (2.1)$$

The parameter η is proportional to time, although it can also be interpreted as the inverse temperature in statistical physics. For Hamiltonians whose classical counterpart is a scalar in phase space, the \hbar expansion of the propagator (2.1) is well known [46]. In fact, for this case the final objective being the \hbar expansion of the density matrix, there are a number of procedures which provide the same result: for instance, the partition function approach of Bhaduri and collaborators [47], the Kirzhnits expansion [28], the algebraic method of Grammaticos and Voros based on the Wigner transform of operators [48], or the direct expansion of the density matrix $\hat{\rho} = \Theta(\lambda - \hat{H})$ [46].

However, in problems where the Hamiltonian has matrix components, as in the relativistic case, the task is more complicated due to the additional difficulty of the non-commutativity of the matrices entering \hat{H} . In this case, the above-mentioned methods are not suitable because they yield an infinite series in powers of η separately for each order of the \hbar expansion of \hat{G} and mix positive and negative energy states, producing strong cancellations in the series. Therefore, to obtain the required \hbar expansion, one has to be capable of resumming the power series of η for the positive and negative energy solutions independently. Hence the interest in finding an alternative and more direct way of obtaining the \hbar expansion.

2.1. Outline of the Method

Consider a time-independent single-particle Hamiltonian \hat{H} which has a matrix structure. The Bloch equation for the propagator is obtained from Eq. (2.1) by differentiation with respect to η :

$$\frac{\partial \hat{G}}{\partial \eta} = -\hat{H}\hat{G} = -\hat{G}\hat{H}. \quad (2.2)$$

To perform the semiclassical approximation of the Bloch equation it is convenient to write Eq. (2.2) symmetrically as

$$\frac{\partial \hat{G}}{\partial \eta} + \frac{1}{2} \{ \hat{H}, \hat{G} \} = 0, \quad (2.3)$$

where $\{ \hat{H}, \hat{G} \}$ is the anticommutator of \hat{H} and \hat{G} . The differential equation (2.3) has to be solved preserving the boundary condition $\hat{G}(\eta=0) = I$, where I is the unit matrix. The Wigner transform [46] of Eq. (2.3) results in

$$\frac{\partial G_w}{\partial \eta} + \frac{1}{2} \left\{ H_w, \exp\left(\frac{i\hbar}{2} \tilde{A}\right), G_w \right\} = 0, \quad (2.4)$$

where A_w denotes the Wigner transform of the operator \hat{A} and the shorthand notation $\{A, C, B\}$ stands for $ACB + BCA$. Use has been made of the following property of the Wigner transform of a product of operators:

$$(\hat{A}\hat{B})_w = A_w \exp\left(\frac{i\hbar}{2} \tilde{A}\right) B_w, \quad (2.5)$$

with $\tilde{A} \equiv \bar{\nabla}_r \cdot \bar{\nabla}_p - \bar{\nabla}_p \cdot \bar{\nabla}_r$ (the arrows indicate the direction in which the gradients act).

If in Eq. (2.4) the Wigner transform of the propagator is explicitly written as a power series of \hbar ,

$$G_w = \sum_{n=0} \hbar^n G_n, \quad (2.6)$$

by expanding $\exp(i\hbar\tilde{A}/2)$ and equating the coefficients of the same powers of \hbar , a set of coupled differential equations for the G_n in the \hbar expansion of the propagator is obtained. These equations can be integrated recurrently by a simple algorithm [39, 40] to yield

$$G_n = -\frac{1}{2} G_0^{1/2} \left[\sum_{m=1}^n \frac{1}{m!} \left(\frac{i}{2}\right)^m \int_0^\eta d\eta' G_0^{-1/2} \{ H_w, (\tilde{A})^m, G_{n-m} \} G_0^{-1/2} \right] G_0^{1/2}. \quad (2.7)$$

One therefore ends up with a recurrence relation in which any desired G_n in the \hbar expansion of the propagator can be obtained starting from the lowest order,

$$G_0 = \exp(-\eta H_w). \quad (2.8)$$

The problem is thus reduced to an algebraic question whose main complexity is the calculation of the symmetric action of the powers of \tilde{A} between H_w and the lower G_n . The use of the propagator has the advantage that it not only yields the density matrix as shown below, but if η is interpreted as an inverse temperature, it also yields the statistical operator, which is represented by \hat{G} apart from a normalizing factor.

2.2. Application to the Relativistic Nuclear Problem

The aim here is to apply the method outlined above to obtain the semiclassical expansion up to order \hbar^2 of the propagator associated with a scalar-vector Dirac Hamiltonian. This Hamiltonian describes the single-particle motion of a set of fermions submitted to a scalar field $S(\mathbf{r})$ and to the time-like component $V(\mathbf{r})$ of a four-vector field, as in the case of relativistic mean field $\sigma - \omega$ models. Defining an effective mass

$$m^*(\mathbf{r}) = m + S(\mathbf{r}), \quad (2.9)$$

such a Hamiltonian reads

$$\hat{H} = \boldsymbol{\alpha} \cdot \hat{\mathbf{p}} + \beta m^*(\mathbf{r}) + IV(\mathbf{r}), \quad (2.10)$$

where $\boldsymbol{\alpha}$ and β are the standard 4×4 Dirac matrices [49] (bold-faced symbols indicate vectors in a three-dimensional space, and we set $\hbar = c = 1$, henceforth, unless \hbar is written explicitly for the sake of clarity in the semiclassical expansions).

As shown in Appendix A, the Wigner transform of the Dirac Hamiltonian (2.10) is

$$H_w = \boldsymbol{\alpha} \cdot \mathbf{p} + \beta m^*(\mathbf{r}) + IV(\mathbf{r}). \quad (2.11)$$

In this case the lowest order of the propagator, Eq. (2.8), takes a simple form [39]

$$G_0 = \left[I \cosh \eta \varepsilon - \frac{\sinh \eta \varepsilon}{\varepsilon} (\boldsymbol{\alpha} \cdot \mathbf{p} + \beta m^*) \right] \exp(-\eta V), \quad (2.12)$$

with $\varepsilon = (p^2 + m^{*2})^{1/2}$. Since the hyperbolic functions which appear in (2.12) can be written in terms of $\exp(-\eta \varepsilon)$ and $\exp(+\eta \varepsilon)$, it is clearly seen that G_0 contains *the positive and negative energy solutions separately*. In addition, all the contributions coming from the expansion of the exponential in Eq. (2.1) in powers of η have been consistently resummed. From the structure of Eq. (2.7), it is evident that these two features of G_0 are kept to any order G_n in the \hbar expansion of the propagator. These are the main advantages of this method in comparison with other alternatives, such as the Kirzhnits method or the direct expansion of the Wigner transform of the Bloch propagator (2.1).

It is worth noting that, in the cases where \hat{H} does not have a matrix structure,

ordinarily there is no term of first order in \hbar in the expansion of the propagator [46]. On the other hand, if the Hamiltonian contains matrices which do not commute, as in the present case, there appear odd powers of \hbar . However, these terms have zero trace and do not contribute to the physical quantities of interest, as will be seen later.

Starting from (2.12), the explicit evaluation of G_1 and G_2 using Eq. (2.7) is in principle straightforward and it has been done by developing a REDUCE computer code to handle the calculations. Further details of the intermediate steps of the calculations or the final expressions for G_1 and G_2 , which involve the gradients of the fields V and S , are not given here. Instead, Appendix B gives the corresponding terms of the semiclassical density matrix which is closely related to the propagator, as described below.

Before closing this subsection, it may be appropriate to say a few words about other ways of performing semiclassical expansions of the relativistic nuclear problem which have appeared during the course of this work. The authors of Refs. [31, 43, 45] start from the equation of motion of the Green's function

$$(i\gamma^0 \partial_0 - \gamma^0 \hat{H}) G_F(x, x') = \delta^4(x - x'), \quad (2.13)$$

where \hat{H} is a Dirac Hamiltonian (notation as in [49]). Expansion of G_F into a formal power series of \hbar , $G_F(x, x') = \sum_n \hbar^n G_F^{(n)}(x, x')$, followed by a Fourier transform of $G_F^{(n)}(x, x')$ [31, 45] or by a Wigner transform of the Dyson equation [43], leads to a recurrence relation which can be solved iteratively to obtain the $G_F^{(n)}(x, x')$. Observables such as the particle density are then obtained from the well-known identity

$$\rho(\mathbf{r}) = -i \lim_{x' \rightarrow x} \text{Tr}[\gamma^0 G_F(x, x')]. \quad (2.14)$$

The relationship between the Green's function and the Bloch propagator (2.1) is indirect (stemming from different boundary conditions):

$$G_F = -i[\Theta(t - t') A^+ - \Theta(t' - t) A^-] \gamma^0 \hat{G}(it - it'). \quad (2.15)$$

In (2.15) $A^\pm = \sum_n |\chi_n^\pm\rangle \langle \chi_n^\pm|$ are the projection operators on positive and negative energy states, with $\hat{H} |\chi_n^\pm\rangle = E_n^\pm |\chi_n^\pm\rangle$. Of course, all necessary information is contained in both propagators G_F and \hat{G} .

2.3. The Wigner-Kirkwood Relativistic Density Matrix

The generalized density matrix $\hat{\mathcal{H}}$ is obtained from the propagator \hat{G} by an inverse Laplace transform (see, e.g., [46]):

$$\hat{\mathcal{H}}(\lambda) = \frac{1}{2\pi i} \int_{c-i\infty}^{c+i\infty} d\eta \exp(\eta\lambda) \frac{\hat{G}(\eta)}{\eta} = \mathcal{L}_{\eta \rightarrow \lambda}^{-1} \left[\frac{\hat{G}(\eta)}{\eta} \right], \quad (2.16)$$

where λ is the chemical potential.

Inserting the \hbar expansion of the propagator into (2.16), one finds the expression of the corresponding WK density matrix:

$$\mathcal{R}_w = \mathcal{L}_{\eta \rightarrow \lambda}^{-1} \left[\frac{G_w(\eta)}{\eta} \right] = \mathcal{R}_0 + \hbar \mathcal{R}_1 + \hbar^2 \mathcal{R}_2 + \dots \quad (2.17)$$

From the definitions of the Laplace transform of the step function and of the derivative of a Laplace transform [50], one formally obtains

$$\mathcal{L}_{\eta \rightarrow \lambda}^{-1} \left[\eta^n \frac{\exp\{-\eta(V \pm \varepsilon)\}}{\eta} \right] = \frac{\partial^n}{\partial \lambda^n} \Theta(\lambda - V \mp \varepsilon). \quad (2.18)$$

Accordingly, the 4×4 relativistic density matrix \mathcal{R}_w will contain the step function, the delta function, and its derivatives. As happens in the non-relativistic problem, \mathcal{R}_w has to be considered as a distribution rather than as a function, in the sense that it is only meaningful if used under an integral sign to compute expectation values of one-body operators.

The zero-order term of the density matrix, cf. Eq. (2.12), is

$$\begin{aligned} \mathcal{R}_0 = & \frac{\Theta(\lambda^+ - V - \varepsilon)}{2} \left[I + \frac{1}{\varepsilon} (\mathbf{a} \cdot \mathbf{p} + \beta m^*) \right] \\ & + \frac{\Theta(\lambda^- - V + \varepsilon)}{2} \left[I - \frac{1}{\varepsilon} (\mathbf{a} \cdot \mathbf{p} + \beta m^*) \right], \end{aligned} \quad (2.19)$$

where the first line corresponds to the positive energy states and the second line to the negative ones. It is indicated that the chemical potentials λ^+ and λ^- may be different in the two cases. Using Eqs. (2.17) and (2.18), \mathcal{R}_1 and \mathcal{R}_2 are directly obtained from G_1 and G_2 , respectively. Their expressions are given in Appendix B.

An interesting property of the density matrix $\hat{\mathcal{R}}$ is its idempotency [46], which holds for the positive ($\hat{\mathcal{R}}^+$) and negative ($\hat{\mathcal{R}}^-$) energy solutions¹ separately:

$$(\hat{\mathcal{R}}^\pm)^2 = \hat{\mathcal{R}}^\pm. \quad (2.20)$$

One can take the Wigner transform of this equation, apply (2.5) to its l.h.s. and then insert the \hbar expansion (2.17) of the density matrix. Regrouping the terms of the same order in \hbar , a set of relationships is found which must be fulfilled by each order of the semiclassical expansion of the density matrix, independently for positive and negative energy solutions. Equation (2.20) yields the following three relations up to order \hbar^2 :

$$\begin{aligned} \mathcal{R}_0^\pm &= \mathcal{R}_0^{\pm 2}, \\ \mathcal{R}_1^\pm &= \{\mathcal{R}_0^\pm, \mathcal{R}_1^\pm\} + \frac{i}{2} \mathcal{R}_0^\pm \tilde{\mathcal{A}} \mathcal{R}_0^\pm, \\ \mathcal{R}_2^\pm &= \mathcal{R}_1^{\pm 2} + \{\mathcal{R}_0^\pm, \mathcal{R}_2^\pm\} + \frac{i}{2} \{\mathcal{R}_0^\pm, \tilde{\mathcal{A}}, \mathcal{R}_1^\pm\} - \frac{1}{8} \mathcal{R}_0^\pm \tilde{\mathcal{A}}^2 \mathcal{R}_0^\pm. \end{aligned} \quad (2.21)$$

¹ Observe that although the density matrix $\hat{\mathcal{R}}^+$ and the projection operators \mathcal{A}^+ introduced in Eq. (2.15) are closely related, they should not be confused since $\hat{\mathcal{R}}^+ = \sum_n |\chi_n^+\rangle \langle \chi_n^+| \Theta(\lambda^+ - E_n^+)$.

Equation (2.21) constitutes a stringent test of the correctness of the calculated semiclassical density matrix.

The results obtained for the \hbar^2 -order relativistic density matrix have been checked to make sure they satisfy (2.21). In the case of the Dirac Hamiltonian, this is an extremely lengthy proof and it is not given here (again the calculations were performed with REDUCE software). Nevertheless, an outline of the procedure is presented in Appendix C, where proof is given that the well-known WK expansion of the local density matrix for a non-relativistic Hamiltonian [51] fulfils (2.21).

3. SEMICLASSICAL RELATIVISTIC PARTICLE AND ENERGY DENSITIES

The semiclassical relativistic density matrix obtained in the preceding section is now used to calculate the \hbar expansion of the particle and energy densities in both the WK approach and the energy density (RETF) formalism.

For a given single-particle operator \hat{O} , its expectation value is defined as

$$\langle \hat{O} \rangle = \frac{1}{(2\pi)^3} \int d\mathbf{r} \int d\mathbf{p} \text{Tr}^+ [\hat{O}(\mathbf{r}, \hat{\mathbf{p}}) \hat{\mathcal{H}}(\mathbf{r}, \hat{\mathbf{p}})]_{\text{w}}, \quad (3.1)$$

where Tr^+ means that the trace is taken disregarding the negative energy terms. Thus, here and in the following only the positive energy solutions are considered; i.e., we restrict ourselves to the positive energy part of the spectrum and neglect the contributions from antiparticles, as is currently done in most applications of relativistic mean field theory. In the case of the operators \hat{O} that will be considered in this section, the semiclassical expectation value corresponding to Eq. (3.1) reduces to

$$\langle \hat{O} \rangle_{\text{sc}} = \frac{1}{(2\pi)^3} \int d\mathbf{r} \int d\mathbf{p} \text{Tr}^+ [O_{\text{w}}(\mathcal{H}_0 + \hbar^2 \mathcal{H}_2)] \quad (3.2)$$

up to order \hbar^2 , since the other terms which in principle could contribute turn out to be zero or vanish after angular averaging in momentum space. This fact was expected for contributions of order \hbar , as we are dealing with a static approximation and the nuclear ground state is invariant under time reversal.

3.1. Wigner-Kirkwood Expressions

Assuming that the integrands are invariant under rotations in momentum space and introducing the local Fermi momentum

$$k_{\text{F}} = [(\lambda - V)^2 - m^{*2}]^{1/2} \quad (3.3)$$

and the definitions

$$\begin{aligned}\varepsilon_F &= \lambda - V = (k_F^2 + m^{*2})^{1/2} \\ x_F &= \varepsilon_F/k_F,\end{aligned}\tag{3.4}$$

the WK particle $\rho(\mathbf{r})$, energy $e(\mathbf{r})$, and kinetic energy $\tau(\mathbf{r})$ densities to order \hbar^2 for each kind of nucleon are found to be:

$$\rho(\mathbf{r}) = \frac{1}{(2\pi)^3} \int d\mathbf{p} \operatorname{Tr}^+ [\hat{\mathcal{H}}(\mathbf{r}, \hat{\mathbf{p}})]_{\mathbf{w}} = \rho_0 + \rho_2,\tag{3.5}$$

$$\rho_0 = k_F^3/3\pi^2,\tag{3.6}$$

$$\begin{aligned}\rho_2 &= \frac{1}{24\pi^2} \left[\frac{1}{k_F} (3 - x_F^2)(\nabla V)^2 - \left(2x_F + 4 \ln \frac{k_F + \varepsilon_F}{m^*} \right) \Delta V \right. \\ &\quad \left. + 2 \frac{x_F}{m^*} (3 - x_F^2)(\nabla V \cdot \nabla m^*) + \frac{1}{k_F} (2 - x_F^2)(\nabla m^*)^2 \right. \\ &\quad \left. + 2 \frac{k_F}{m^*} (1 - x_F^2) \Delta m^* \right];\end{aligned}\tag{3.7}$$

$$\begin{aligned}e(\mathbf{r}) &= \frac{1}{(2\pi)^3} \int d\mathbf{p} \operatorname{Tr}^+ [(\boldsymbol{\alpha} \cdot \hat{\mathbf{p}} + \beta m^*(\mathbf{r}) + IV(\mathbf{r})) \hat{\mathcal{H}}(\mathbf{r}, \hat{\mathbf{p}})]_{\mathbf{w}} \\ &= e_0 + e_2,\end{aligned}\tag{3.8}$$

$$e_0 = \frac{1}{8\pi^2} \left[k_F \varepsilon_F^3 + k_F^3 \varepsilon_F - m^{*4} \ln \frac{k_F + \varepsilon_F}{m^*} \right] + V\rho_0,\tag{3.9}$$

$$\begin{aligned}e_2 &= \frac{1}{24\pi^2} \left[\left(x_F(2 - x_F^2) - 2 \ln \frac{k_F + \varepsilon_F}{m^*} \right) (\nabla V)^2 \right. \\ &\quad \left. - 2k_F(1 + x_F^2) \Delta V + 2 \frac{m^*}{k_F} (1 - x_F^2)(\nabla V \cdot \nabla m^*) \right. \\ &\quad \left. + \left(x_F(1 - x_F^2) - \ln \frac{k_F + \varepsilon_F}{m^*} \right) (\nabla m^*)^2 \right. \\ &\quad \left. - 2m^* \left(x_F - \ln \frac{k_F + \varepsilon_F}{m^*} \right) \Delta m^* \right] + V\rho_2;\end{aligned}\tag{3.10}$$

and

$$\tau(\mathbf{r}) = \frac{1}{(2\pi)^3} \int d\mathbf{p} \operatorname{Tr}^+ [(\boldsymbol{\alpha} \cdot \hat{\mathbf{p}} + \beta m - Im) \hat{\mathcal{H}}(\mathbf{r}, \hat{\mathbf{p}})]_{\mathbf{w}} = \tau_0 + \tau_2,\tag{3.11}$$

$$\begin{aligned}\tau_0 &= \frac{1}{8\pi^2} \left[2k_F \varepsilon_F^3 - m^{*2} \left(5 - 4 \frac{m}{m^*} \right) k_F \varepsilon_F + m^{*4} \left(3 - 4 \frac{m}{m^*} \right) \ln \frac{k_F + \varepsilon_F}{m^*} \right] - m\rho_0,\end{aligned}\tag{3.12}$$

$$\begin{aligned}
\tau_2 = & \frac{1}{24\pi^2} \left\{ \left[\left(3 - (1 + x_F^2) \frac{m}{m^*} \right) x_F - 2 \ln \frac{k_F + \varepsilon_F}{m^*} \right] (\nabla V)^2 \right. \\
& - 2k_F \left[2 - (1 - x_F^2) \frac{m}{m^*} \right] \Delta V \\
& - 2 \left[\frac{m}{k_F} (2 + x_F^2) + 3 \frac{k_F}{m^*} (1 - x_F^2) \right] (\nabla V \cdot \nabla m^*) \\
& + \left[\left(3 - 2 \frac{m}{m^*} \right) x_F - \frac{m}{m^*} x_F^3 - \ln \frac{k_F + \varepsilon_F}{m^*} \right] (\nabla m^*)^2 \\
& \left. - 2m \left[x_F - \left(3 - 2 \frac{m^*}{m} \right) \ln \frac{k_F + \varepsilon_F}{m^*} \right] \Delta m^* \right\} - m\rho_2. \quad (3.13)
\end{aligned}$$

Equations (3.6), (3.9), and (3.12) correspond to the \hbar^0 -order WK approach, whereas Eqs. (3.7), (3.10), and (3.13) are the respective \hbar^2 -order WK corrections. In view of (3.2), the scalar density

$$\rho_s(\mathbf{r}) = \frac{1}{(2\pi)^3} \int d\mathbf{p} \operatorname{Tr}^+ [\beta \hat{\mathcal{H}}(\mathbf{r}, \hat{\mathbf{p}})]_w \quad (3.14)$$

can be computed from the foregoing expressions:

$$\rho_s(\mathbf{r}) = \frac{1}{m^* - m} [e - \tau - (m + V) \rho]. \quad (3.15)$$

It is worthwhile indicating that in the case of applications, where the self-energy operator is determined from a many-body calculation, a term

$$\frac{1}{2} [\beta S(\mathbf{r}) + IV(\mathbf{r})] \quad (3.16)$$

should be subtracted from the Hamiltonian to avoid double counting of the meson contributions to the energy. In this case the energy density would become

$$\frac{1}{2} [e(\mathbf{r}) + \tau(\mathbf{r}) + m\rho(\mathbf{r})]. \quad (3.17)$$

These equations complete the results published in [39] and correct some misprints which appeared there. In the mean field approximation, the expressions for ρ and e obtained by Speicher, Dreizler, and Engel [45], using the Green's function formalism, and by Von-Eiff, Haddad, and Weigel [52], from the Wigner transformed Dyson equation, are identical to the results given here. Even though the interested reader could certainly obtain ρ and e as given above from the results published in [45], they have been recorded here for the sake of completeness and

to make the discussion about the relativistic density functionals, which comes in Section 3.2, fully understandable.

Setting $m^* = m$ in the above equations one recovers the expressions for the atomic case [30]. The non-relativistic limit of the particle and kinetic energy densities has also been examined. One has to expand the above equations in powers of k_F/m^* , retain the lowest orders, and finally expand $(m^*)^n = m^n(1 + S/m)^n$ in terms of S/m . This yields the standard non-relativistic formulae for ρ and τ [46] for a set of fermions moving in a potential well, which in this case is the sum $V + S$ of the meson potentials.

3.2. Density Functionals

To obtain the RETF density functionals one has to write ∇V and ΔV as a function of the particle density, the effective mass, and their gradients, and insert them into the \hbar^2 terms of the WK expansions. This is first achieved by putting the expression (3.3) of k_F in terms of V in Eq. (3.6)

$$\rho_0 = \frac{1}{3\pi^2} [(\lambda - V)^2 - m^{*2}]^{3/2}, \quad (3.18)$$

and then computing ∇V and ΔV from this equation. In the next step, as one works with the density ρ rather than with ρ_0 , ρ is expanded about a new variable k_0 up to order \hbar^2 ,

$$\rho(k_F) = \rho_0(k_0) + \left(\frac{\partial \rho_0(k_0)}{\partial k_0} \right) \delta k + \rho_2(k_0) + \mathcal{O}(\hbar^4), \quad (3.19)$$

where $\delta k = k_F - k_0$ and ρ_2 is defined in (3.7). One then requires that $\rho_0(k_0)$ reproduces the exact density,

$$\rho_0(k_0) = \rho(k_F), \quad (3.20)$$

whence it follows that

$$k_F = k_0 \left[1 - \frac{\pi^2}{k_0^3} \rho_2(k_0) \right] \quad (3.21)$$

to order \hbar^2 . Then one substitutes in the WK expressions of order \hbar^0 for k_F as given by (3.21) and expands these equations about the value k_0 consistently to order \hbar^2 . Finally, k_0 is replaced by k_F , with $k_F = (3\pi^2\rho)^{1/3}$. Following this procedure, the scalar, energy, and kinetic energy density functionals in the RETF formalism, including \hbar^2 -order corrections, are obtained:

$$\begin{aligned}
\rho_s(\mathbf{r}) = & \frac{m^*}{2\pi^2} \left[k_F \varepsilon_F - m^{*2} \ln \frac{k_F + \varepsilon_F}{m^*} \right] \\
& - \frac{1}{72\varepsilon_F^2} \left[\left(\frac{\varepsilon_F}{m^*} \left(2 + 3 \frac{m^{*2}}{\varepsilon_F^2} \right) - 4 \frac{m^*}{k_F} \left(2 - \frac{m^{*2}}{\varepsilon_F^2} \right) \ln \frac{k_F + \varepsilon_F}{m^*} \right) \frac{(\nabla\rho)^2}{\rho} \right. \\
& + 12 \frac{m^*}{k_F} \ln \frac{k_F + \varepsilon_F}{m^*} \Delta\rho - \frac{6}{k_F} \left(3 \frac{k_F}{\varepsilon_F} + 4 \frac{m^{*2}}{\varepsilon_F^2} \ln \frac{k_F + \varepsilon_F}{m^*} \right) (\nabla\rho \cdot \nabla m^*) \\
& + \frac{9}{m^* k_F} \left(3 \frac{k_F}{\varepsilon_F} + 4 \frac{m^{*2}}{\varepsilon_F^2} \ln \frac{k_F + \varepsilon_F}{m^*} \right) \rho (\nabla m^*)^2 \\
& \left. + \frac{18}{k_F} \left(\frac{\varepsilon_F}{k_F} - \left(2 + \frac{\varepsilon_F^2}{k_F^2} \right) \ln \frac{k_F + \varepsilon_F}{m^*} \right) \rho \Delta m^* \right]; \quad (3.22)
\end{aligned}$$

$$\begin{aligned}
e(\mathbf{r}) = & \frac{1}{8\pi^2} \left[k_F \varepsilon_F^3 + k_F^3 \varepsilon_F - m^{*4} \ln \frac{k_F + \varepsilon_F}{m^*} \right] \\
& + \frac{1}{72\varepsilon_F^2} \left[\left(\varepsilon_F + 2k_F \ln \frac{k_F + \varepsilon_F}{m^*} \right) \frac{(\nabla\rho)^2}{\rho} + 12 \frac{m^*}{k_F} \ln \frac{k_F + \varepsilon_F}{m^*} (\nabla\rho \cdot \nabla m^*) \right. \\
& \left. + \frac{9}{k_F} \left(\frac{\varepsilon_F}{k_F} - \left(2 + \frac{\varepsilon_F^2}{k_F^2} \right) \ln \frac{k_F + \varepsilon_F}{m^*} \right) \rho (\nabla m^*)^2 \right] + V\rho; \quad (3.23)
\end{aligned}$$

and

$$\begin{aligned}
\tau(\mathbf{r}) = & \frac{1}{8\pi^2} \left[2k_F \varepsilon_F^3 - m^{*2} \left(5 - 4 \frac{m}{m^*} \right) k_F \varepsilon_F + m^{*4} \left(3 - 4 \frac{m}{m^*} \right) \ln \frac{k_F + \varepsilon_F}{m^*} \right] \\
& + \frac{1}{72\varepsilon_F^2} \left\{ \left[\varepsilon_F + \varepsilon_F \left(1 - \frac{m}{m^*} \right) \left(2 - \frac{m^{*2}}{\varepsilon_F^2} \right) \right. \right. \\
& + 2k_F \left(1 + 2 \left(1 - \frac{m}{m^*} \right) \frac{m^{*2}}{\varepsilon_F^2} \right) \ln \frac{k_F + \varepsilon_F}{m^*} \left. \right] \frac{(\nabla\rho)^2}{\rho} \\
& + 12 \frac{m^*}{k_F} \left(1 - \frac{m}{m^*} \right) \left[\frac{k_F}{\varepsilon_F} - \left(1 - 2 \frac{m^{*2}}{\varepsilon_F^2} \right) \ln \frac{k_F + \varepsilon_F}{m^*} \right] (\nabla\rho \cdot \nabla m^*) \\
& - \frac{9}{k_F} \left[\frac{\varepsilon_F}{k_F} + 3 \left(1 - \frac{m}{m^*} \right) \frac{k_F}{\varepsilon_F} \right. \\
& \left. \left. - \left(2 + \frac{\varepsilon_F^2}{k_F^2} - 4 \left(1 - \frac{m}{m^*} \right) \frac{m^{*2}}{\varepsilon_F^2} \right) \ln \frac{k_F + \varepsilon_F}{m^*} \right] \rho (\nabla m^*)^2 \right\} - m\rho. \quad (3.24)
\end{aligned}$$

Note that Eqs. (3.23) and (3.24) take this form after partial integration of the terms with $\Delta\rho$ and Δm^* .

If one takes $m^* = m$, Eq. (3.24) reduces to the result of atomic physics [30]. In the non-relativistic limit ($k_F \ll m$, $S \ll m$) the well-known result

$$\tau = \tau_0 + \tau_2 = \frac{3}{10m} (3\pi^2)^{2/3} \rho^{5/3} + \frac{1}{72m} \frac{(\nabla \rho)^2}{\rho} \quad (3.25)$$

is obtained from (3.24). In fact, taking the limit before the elimination of the Laplacians in (3.24) by partial integration, the usual term $\Delta \rho / 6m$ is also found.

We would like to point out that the inversion scheme used here to derive the density functionals from the WK expansions is not the only possibility which can be considered. An alternative elimination arises if an additional inversion of the effective mass at order \hbar^0 is also performed [45]. However, in the scheme adopted here the effective mass is treated in a parallel way to that used in the non-relativistic case, where no supplementary inversion of m^* is carried out (see, e.g., [48, 53]). We shall not dwell here any further on this point; but will return to it in Section 5 when the $\sigma - \omega$ model is studied. It will be shown there that the variational Euler-Lagrange equations obtained from both inversion schemes turn out to be equivalent.

To conclude this section, it is worth mentioning that the semiclassical expansions formulated here are asymptotic by nature and are not expected to converge a priori. Nevertheless, one trusts that such expansions truncated at the lowest orders provide both reliable and sufficiently accurate numerical results, as happens in the non-relativistic case. The applications investigated in the following sections will show that this is also the case in the relativistic regime.

4. RESULTS FOR A RELATIVISTIC HARMONIC OSCILLATOR

The harmonic oscillator potential has been extensively studied and has found many applications in non-relativistic nuclear physics. In this section a relativistic harmonic oscillator model is used to investigate quantitatively the accuracy of the semiclassical approximations deduced above.

We shall consider the situation where the scalar field and the zero component of the vector field correspond to a three-dimensional spherically symmetric harmonic oscillator:

$$S(r) = V(r) = \frac{1}{2} K r^2. \quad (4.1)$$

In this case the Dirac equation can be solved analytically [54, 55] (other types of Dirac equation with an oscillator potential which admit analytical solutions are found in the literature [56]). Here the semiclassical WK and RETF results will be compared with the quantal ones and also with the corresponding Strutinsky averaged calculation.

4.1. Solution of the Dirac Equation

If the Dirac spinor is written as

$$\psi = \begin{pmatrix} \varphi_u \\ \varphi_d \end{pmatrix} e^{-iEt}, \quad (4.2)$$

the Dirac equation associated with the static scalar and vector potentials (4.1) for the large φ_u and small φ_d components reads

$$(m + 2V) \varphi_u + (\boldsymbol{\sigma} \cdot \hat{\mathbf{p}}) \varphi_d = E \varphi_u, \quad (4.3)$$

$$(\boldsymbol{\sigma} \cdot \hat{\mathbf{p}}) \varphi_u - m \varphi_d = E \varphi_d. \quad (4.4)$$

Combining (4.3) and (4.4), the Dirac equation transforms into a Schrödinger-like equation for the large component φ_u with an energy-dependent potential [54, 55]

$$\left(\frac{\hat{p}^2}{2m} + \frac{E + m}{m} V \right) \varphi_u = \frac{E^2 - m^2}{2m} \varphi_u, \quad (4.5)$$

and the small component φ_d is obtained from φ_u through (4.4),

$$\varphi_d = \frac{1}{E + m} (\boldsymbol{\sigma} \cdot \hat{\mathbf{p}}) \varphi_u. \quad (4.6)$$

Unlike Ref. [55], the problem is solved here without neglecting the mass of the particle. The Dirac spinor (4.2) is rewritten as

$$\psi_{nljm} = \begin{pmatrix} ig_{nl}/r \\ f_{nl}/r^2 (\boldsymbol{\sigma} \cdot \mathbf{r}) \end{pmatrix} \varphi_{ljm} e^{-iE_{nl}t}, \quad (4.7)$$

where

$$\varphi_{ljm} = \sum_{m_l, m_s} \langle l \frac{1}{2} m_l m_s | jm \rangle Y_{l, m_l}(\hat{\mathbf{r}}) \chi_{1/2, m_s}, \quad (4.8)$$

and the normalization is

$$\int_0^\infty dr (g^2 + f^2) = 1. \quad (4.9)$$

By standard techniques, the solution to (4.5) is easily found to be

$$g_{nl}(r) = N_{nl} r \left(\frac{r}{r_0} \right)^l \exp(-r^2/2r_0^2) L_n^{l+1/2} \left(\frac{r^2}{r_0^2} \right), \quad (4.10)$$

where $L_n^x(x)$ are the generalized Laguerre polynomials [50]. Evaluation of (4.6) from (4.10) yields

$$f_{nl}(r) = -\frac{N_{nl}}{E_{nl} + m} \left(\frac{r}{r_0} \right)^{l+2} \exp(-r^2/2r_0^2) \left[L_n^{l+3/2} \left(\frac{r^2}{r_0^2} \right) + L_n^{l+5/2} \left(\frac{r^2}{r_0^2} \right) \right] \quad (4.11)$$

for $j = l + \frac{1}{2}$, and

$$f_{nl}(r) = \frac{N_{nl}}{E_{nl} + m} \left(\frac{r}{r_0} \right)^l \exp(-r^2/2r_0^2) \times \left[\left(n + l - \frac{1}{2} \right) L_n^{l-1/2} \left(\frac{r^2}{r_0^2} \right) + n L_n^{l-1/2} \left(\frac{r^2}{r_0^2} \right) \right] \quad (4.12)$$

for $j = l - \frac{1}{2}$. The normalization factor is

$$N_{nl} = \frac{1}{r_0} \left[\frac{4(n-1)! (E_{nl} + m)}{r_0 \Gamma(n + l + 1/2) (3E_{nl} + m)} \right]^{1/2}. \quad (4.13)$$

The energy eigenvalue is obtained from

$$(E_{nl} - m)(E_{nl}^2 - m^2) = 4K(2n + l - \frac{1}{2})^2 \quad (4.14)$$

and the scale parameter r_0 is

$$r_0 = \frac{1}{[K(E_{nl} + m)]^{1/4}}, \quad (4.15)$$

with $n = 1, 2, 3, \dots$ and $l = 0, 1, 2, \dots$. Note that E is independent of j (the spin-orbit couplings arising from the scalar field and from the vector field cancel each other) and that r_0 depends on the state (n, l) . A given oscillator shell can be characterized by a quantum number N such that $N = 2n + l - 2$. In the ultrarelativistic limit, $E_N \gg m$, the result of Ref. [55] is obtained,

$$E_N = [2K^{1/2}(N + \frac{3}{2})]^{2/3}, \quad (4.16)$$

and in the non-relativistic limit, $E_N - m \ll m$,

$$E_N = \left(N + \frac{3}{2} \right) \left(\frac{2K}{m} \right)^{1/2} + m. \quad (4.17)$$

For A non-interacting particles moving in an external harmonic oscillator (4.1), the quantal particle density $\rho(r)$ and total energy E are obtained from Eqs. (4.10)–(4.12) and (4.14), respectively, by summing over the occupied states.

4.2. Wigner–Kirkwood Expansion of the Particle Number and the Energy

In the WK representation the semiclassical particle and energy densities, Eqs. (3.5)–(3.7) and (3.8)–(3.10), become (assuming isospin degeneracy and taking into account the fact that $\nabla m^* = \nabla V$ and $\Delta m^* = \Delta V$):

$$\rho_{\text{WK}}(r) = \frac{2}{3\pi^2} k_F^3 + \frac{1}{12\pi^2} \left[\frac{1}{m^* k_F^3} (m^* (3\varepsilon_F^2 - 5m^{*2}) + \varepsilon_F (4\varepsilon_F^2 - 6m^{*2})) (\nabla V)^2 - 2 \left(\frac{1}{k_F} (\varepsilon_F + m^*) + 2 \ln \frac{k_F + \varepsilon_F}{m^*} \right) \Delta V \right], \quad (4.18)$$

$$\begin{aligned}
e_{\text{WK}}(r) = & \frac{1}{4\pi^2} \left[k_F \varepsilon_F (2\varepsilon_F^2 - m^{*2}) - m^{*4} \ln \frac{k_F + \varepsilon_F}{m^*} \right] \\
& + \frac{1}{12\pi^2} \left[\left(\frac{1}{k_F^3} (\varepsilon_F - 2m^*)(\varepsilon_F + m^*)^2 - 3 \ln \frac{k_F + \varepsilon_F}{m^*} \right) (\nabla V)^2 \right. \\
& \left. - 2 \left(\frac{1}{k_F} (\varepsilon_F + m^*)(2\varepsilon_F - m^*) - m^* \ln \frac{k_F + \varepsilon_F}{m^*} \right) \Delta V \right] \\
& + (V - m) \rho_{\text{WK}}, \tag{4.19}
\end{aligned}$$

where k_F is related to the chemical potential λ by

$$k_F = (\lambda + m)^{1/2} (\lambda - m - Kr^2)^{1/2}, \tag{4.20}$$

and $\varepsilon_F = \lambda - Kr^2/2$.

Equations (4.18) and (4.19) can be integrated analytically from $r=0$ to the turning point $r = [(\lambda - m)/K]^{1/2}$ to obtain the semiclassical WK expansion of the particle number and total energy up to order \hbar^2 . With the definition $x \equiv (\lambda - m)/2m$, the following results are found:

$$A = \frac{2}{3} m^3 \left(\frac{2m}{K} \right)^{3/2} (1+x)^{3/2} x^3 - \frac{m}{2} \left(\frac{2m}{K} \right)^{1/2} (1+x)^{1/2} x, \tag{4.21}$$

$$\begin{aligned}
E = & \frac{128}{3465} m^4 \left(\frac{2m}{K} \right)^{3/2} (1+x)^{1/2} \\
& \times \left[\frac{945}{32} x^5 + \frac{2905}{64} x^4 + \frac{1135}{64} x^3 + \frac{3}{8} x^2 - \frac{1}{2} x + 1 - (1+x)^{-1/2} \right] \\
& - \frac{4}{15} m^2 \left(\frac{2m}{K} \right)^{1/2} (1+x)^{1/2} \\
& \times \left[\frac{9}{4} x^2 + \frac{11}{8} x + 1 - (1+x)^{-1/2} \right] - mA. \tag{4.22}
\end{aligned}$$

Equation (4.21) is used to determine the chemical potential λ , which is then inserted into (4.22) to compute the energy. The non-relativistic limit of (4.21) and (4.22) is easily found taking $x \ll 1$. It yields

$$A = \frac{1}{12} \left(\frac{2m}{K} \right)^{3/2} (\lambda - m)^3 - \frac{1}{4} \left(\frac{2m}{K} \right)^{1/2} (\lambda - m), \tag{4.23}$$

$$E = \frac{1}{16} \left(\frac{2m}{K} \right)^{3/2} (\lambda - m)^4 - \frac{1}{8} \left(\frac{2m}{K} \right)^{1/2} (\lambda - m)^2. \tag{4.24}$$

4.3. Discussion of Results

In non-relativistic nuclear physics, the Strutinsky averaging method has been successfully employed to separate the smooth part of the energy from the fluctuating shell corrections [25, 57–59]. The usual prescription for obtaining the smoothed energy uses single-particle occupation numbers, or the single-particle level density, smoothed by some averaging function. We have also performed Strutinsky averaged (SA) calculations for the relativistic harmonic oscillator of Eq. (4.1). Equation (4.14) has been used for the single-particle energies and the smoothed occupation numbers have been obtained by Gaussian averaging. The so-called *plateau condition* (stationarity of the shell correction) [57] has been numerically checked in each case.

For numerical applications K is taken to be $K = m\omega^2/2$, as in the non-relativistic limit the problem then consists of a set of fermions moving in a potential well given by

$$V_{\text{NR}}(r) = V(r) + S(r) = \frac{1}{2}m\omega^2 r^2. \quad (4.25)$$

Table I gives the energies obtained from the SA and semiclassical approaches in comparison with the corresponding quantum mechanical (QM) result for different values of the particle number (closed shells) and of the rest mass of the particles ($m = m_N$, $m = m_N/100$, and $m = m_N/1000$, where $m_N = 939$ MeV), with $\omega = 41A^{-1/3}$ (MeV). The semiclassical energies calculated from the WK expansion of order \hbar^2 are labelled $\text{WK}\hbar^2$ in Table I. The solutions of the Euler-Lagrange equations associated with the RETF energy density functional of order \hbar^2 are labelled $\text{TF}\hbar^2$ (this approach will be discussed below).

For a non-relativistic harmonic oscillator potential, the SA method and the WK expansion up to order \hbar^4 yield the same results and have been shown to be equivalent analytically [57, 58]. Due to the fact that the relativistic eigenvalues (4.14) have a more complicated form than the non-relativistic ones, we have not been able to obtain an analytical expression for the Strutinsky smoothed energy. However, the numerical results shown in Table I seem to indicate that for this relativistic oscillator model the SA and WK methods are also equivalent. The agreement between the SA and $\text{WK}\hbar^2$ energies is almost perfect irrespective of the value of the rest mass of the particles. The small difference between the SA and $\text{WK}\hbar^2$ methods could be attributed to the \hbar^4 contribution which has not been included in the relativistic treatment.

In the QM case, the relativistic effects on the energy are seen to be rather small if the rest mass is the nucleon mass m_N ; the relativistic energy is shifted to smaller values by approximately 1%. The relativistic corrections become more important when the mass is reduced. Compared with the non-relativistic results, which are independent of m , the energy decreases by $\approx 35\%$ if $m = m_N/100$ and by $\approx 64\%$ if $m = m_N/1000$. The SA and semiclassical energies show the same trends as the quantal ones, similar changes are found in their values if the relativistic and non-relativistic results are compared. The difference between the quantal and the SA

TABLE I

Total Energy for a Set of A Fermions Submitted to the Relativistic Harmonic Oscillator (4.1), with $K = m\omega^2/2$, $\omega = 41A^{-1/3}$ (MeV) and $m_N = 939$ MeV

		E (MeV)			
	A	QM	SA	WK \hbar^2	TF \hbar^2
Non-relativistic	16	585.8	598.1	598.1	582.9
	40	1438.6	1454.7	1454.7	1436.1
	80	2854.6	2874.5	2874.5	2852.8
	140	4974.5	4998.2	4998.2	4973.6
	224	7939.2	7966.8	7966.8	7939.4
Relativistic $m = m_N$	16	580.0	592.0	592.0	576.8
	40	1424.5	1439.9	1440.2	1421.8
	80	2826.7	2845.7	2846.1	2824.7
	140	4925.9	4948.8	4949.1	4925.1
	224	7861.7	7888.4	7888.6	7862.2
Relativistic $m = m_N/100$	16	385.4	390.7	391.5	378.7
	40	948.5	955.8	956.4	941.5
	80	1883.7	1893.0	1893.4	1876.7
	140	3284.1	3295.4	3295.6	3277.2
	224	5242.9	5255.9	5256.2	5236.2
Relativistic $m = m_N/1000$	16	207.1	209.7	210.1	202.3
	40	510.4	513.9	514.2	505.3
	80	1014.3	1018.7	1018.9	1009.1
	140	1768.9	1774.2	1774.4	1763.6
	224	2824.4	2830.6	2830.8	2819.2

Note. The results correspond to quantum mechanical (QM), Strutinsky averaged (SA), \hbar^2 -order Wigner-Kirkwood (WK \hbar^2), and Thomas-Fermi (TF \hbar^2) calculations, respectively. The rest mass contribution has been subtracted.

energy is the so-called shell correction. Table I shows that it becomes less important when the mass of the particles is reduced. Thus, the shell correction is reduced by the relativistic effects, at least in this problem.

In the non-relativistic case, the scale parameter r_0 is independent of the energy of the shell but still depends on the mass of the particles and is scaled by a factor $(m_N/m)^{1/2}$. In the relativistic case, r_0 depends both on the mass and on the energy of each shell and becomes smaller as these quantities increase. This causes the relativistic densities to be pushed towards the origin, thus increasing their value at $r=0$ with respect to the non-relativistic case. This effect is clearly observable in Fig. 1, where the relativistic and non-relativistic densities for a harmonic oscillator of $A = 224$ particles with $m = m_N/100$ are plotted for the QM, WK \hbar^2 , and TF \hbar^2 (see below) approaches. In this case the relativistic r_0 is reduced by 80%, and the central density increases roughly by a factor of 2. The smoothing of the oscillations in the quantal density when the relativistic effects are taken into account can also

be seen. This is in agreement with the trend previously found for the shell correction to the energy.

The semiclassical densities show no oscillations since they lack a shell structure. However, they average the quantal densities in the non-relativistic as well as in the relativistic cases. This means that the relativistic effects are properly incorporated by the semiclassical calculation. As happens in the non-relativistic case, the $WK\hbar^2$ semiclassical densities diverge at the classical turning point and, consequently, have to be regarded more as distributions than as functions. In spite of this, the calculation of expectation values of operators is well defined as seen in the case of the particle number (4.21) and the energy (4.22). Note the steep fall-off of the $WK\hbar^2$ densities in Fig. 1; a cutoff has been put at the turning point where they become negative.

The results shown in Table I and Fig. 1 have been obtained with a potential well whose strength K depends on the rest mass m of the particles. Calculations have been carried out changing m but keeping the strength fixed to a constant value $K = K_N \equiv m_N(41A^{-1/3})^2/2$. The corresponding results are displayed in Table II. In this case one finds the same trends as discussed above when the semiclassical results are compared with the quantal results. The excellent agreement between $WK\hbar^2$ and SA should be pointed out.

Finally, we would like to examine the $TF\hbar^2$ results obtained by applying the variational principle to the energy density functional (3.23). The corresponding Euler-Lagrange equation

$$\frac{\delta e}{\delta \rho} = \frac{\partial e}{\partial \rho} - \nabla \cdot \frac{\partial e}{\partial (\nabla \rho)} = \lambda \quad (4.26)$$

has been solved using the imaginary time step method (insight into its practical implementation can be gained from Subsection 5.1.2).

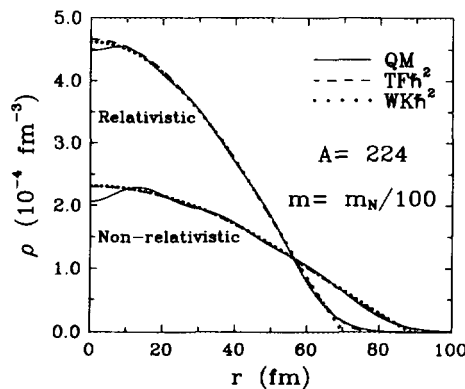


FIG. 1. Particle densities for the relativistic and non-relativistic harmonic oscillators discussed in the text.

TABLE II

Energies as in Table I, but with the Strength of the Potential Kept to a Constant Value $K \approx K_N \equiv m_N(41A^{-1/3})^2/2$

		E (MeV)			
	A	QM	SA	WK \hbar^2	TF \hbar^2
Relativistic $m = m_N/100$	16	2070.7	2096.9	2100.5	2022.9
	40	5103.8	5139.2	5141.9	5053.2
	80	10142.5	10186.9	10189.2	10090.5
	140	17688.7	17742.0	17743.9	17636.1
	224	28243.8	28306.0	28307.7	28191.6
Relativistic $m = m_N/1000$	16	2156.3	2182.2	2186.3	2101.9
	40	5317.5	5353.0	5355.9	5259.8
	80	10569.7	10614.2	10616.6	10510.3
	140	18436.0	18489.4	18491.6	18375.9
	224	29439.3	29501.6	29503.6	29379.3

As in the non-relativistic case, the TF \hbar^2 method is not equivalent to the WK \hbar^2 one (note the difference between the WK \hbar^2 and TF \hbar^2 results in Table I), because they originate from different rearrangements in the \hbar expansion of the energy functional. Consequently, since the WK and SA methods have been shown to be numerically equivalent for this harmonic oscillator model, the smooth part of the energy is not as well estimated by the TF \hbar^2 method. However, the divergence problems in the classically forbidden region are not present in the TF \hbar^2 functionals. This is an advantage of the TF \hbar^2 over the WK \hbar^2 method. The divergent behaviour of WK \hbar^2 at the turning point can be seen in Fig. 2, where the density tails corresponding to Fig. 1 have been plotted on a semi-logarithmic scale.

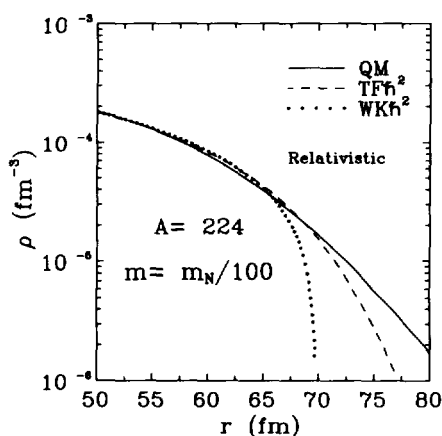


FIG. 2. Semi-logarithmic plot of the density tails corresponding to the relativistic harmonic oscillator of Fig. 1.

From Tables I and II it is seen that the $WK\hbar^2$ and SA methods underbind the system in comparison with the quantal result, regardless of the mass of the particles. This is, of course, expected since shell effects yield additional binding. Nevertheless, the $TF\hbar^2$ approximation generally yields some overbinding.

5. APPLICATION TO FINITE NUCLEI AND SEMI-INFINITE NUCLEAR MATTER

Relativistic extended Thomas–Fermi calculations of finite nuclei in non-linear $\sigma - \omega$ models have been carried out in Ref. [41]. Further RETF results for finite nuclei and also for semi-infinite nuclear matter are presented here. In the first part of this section the binding energies, sizes, and density distributions of finite nuclei calculated in the semiclassical $TF\hbar^0$ and $TF\hbar^2$ approximations are compared with the corresponding Hartree results. For this study two parameter sets different from those employed in [41] have been chosen. Following Ref. [60], they are denominated here by HII [61] and HIV [62]. These parameterizations have effective masses at saturation above $m^*/m \approx 0.60$, which render the $TF\hbar^2$ Klein–Gordon equation associated with the σ meson more stable from a numerical point of view [41]. In the second part of the section the semiclassical liquid drop model coefficients related to the surface and curvature energies are obtained. In addition to HII and HIV, the parameter sets P1 and PW1 (notation as in [63]) are used. P1 was fitted to reproduce ground-state properties of finite nuclei [5], and PW1 corresponds to the original linear Walecka model [2]. Hartree results of surface properties are available for the sets P1 and PW1 [63].

5.1. Finite Nuclei

5.1.1. Lagrangian and Variational Equations

The notation closely follows that of Serot and Walecka [2]. The extended Walecka Lagrangian proposed by Boguta and Bodmer [7], including the electromagnetic field, is

$$\begin{aligned} \mathcal{L} = & \bar{\psi} [\gamma_\mu (i\partial^\mu - g_v V^\mu) - m^*] \psi + \frac{1}{2} (\partial_\mu \phi \partial^\mu \phi - m_s^2 \phi^2) - \frac{1}{3} b \phi^3 - \frac{1}{4} c \phi^4 \\ & - \frac{1}{4} F_{\mu\nu} F^{\mu\nu} + \frac{1}{2} m_v^2 V_\mu V^\mu - \frac{1}{4} H_{\mu\nu} H^{\mu\nu} - e \bar{\psi} \gamma_\mu \frac{1}{2} (1 + \tau_3) A^\mu \psi, \end{aligned} \quad (5.1)$$

where

$$F_{\mu\nu} = \partial_\mu V_\nu - \partial_\nu V_\mu, \quad H_{\mu\nu} = \partial_\mu A_\nu - \partial_\nu A_\mu. \quad (5.2)$$

The effective mass m^* is related to the scalar field ϕ by

$$m^* = m - g_s \phi. \quad (5.3)$$

The σ -meson mass m_s , the coupling constants g_s and g_v , b and c are the free parameters of the Lagrangian, usually chosen to reproduce the properties of nuclear matter and finite nuclei.

The energy density is derived in a standard way from the Lagrangian. In the static Hartree approximation it is given by

$$e^H = \sum_{\alpha} \varphi_{\alpha}^{\dagger} [-i\alpha \cdot \nabla + \beta m^* - m + g_v V_0 + e \frac{1}{2}(1 + \tau_3) A_0] \varphi_{\alpha} + \frac{1}{3} b \phi_0^3 + \frac{1}{4} c \phi_0^4 \\ + \frac{1}{2} [(\nabla \phi_0)^2 + m_s^2 \phi_0^2] - \frac{1}{2} [(\nabla V_0)^2 + m_v^2 V_0^2] - \frac{1}{2} (\nabla A_0)^2, \quad (5.4)$$

where the meson fields have been approximated by their ground-state expectation values and φ_{α} is the single-particle basis in which the nucleon field is expanded. The summation over α is restricted to the occupied bound states of the positive energy spectrum, and now $m^* = m - g_s \phi_0$.

In the semiclassical TF \hbar^2 method one evaluates the energy density from Eq. (3.23):

$$e^{\text{sc}} = e_0 + e_2 - m\rho + g_v V_0 \rho + e A_0 \rho_p + \frac{1}{3} b \phi_0^3 + \frac{1}{4} c \phi_0^4 + \frac{1}{2} [(\nabla \phi_0)^2 + m_s^2 \phi_0^2] \\ - \frac{1}{2} [(\nabla V_0)^2 + m_v^2 V_0^2] - \frac{1}{2} (\nabla A_0)^2, \quad (5.5)$$

with

$$e_0 = \sum_q \frac{1}{8\pi^2} \left[k_F \varepsilon_F^3 + k_F^3 \varepsilon_F - m^{*4} \ln \frac{k_F + \varepsilon_F}{m^*} \right]_q \quad (5.6)$$

and

$$e_2 = \sum_q [B_{1q}(k_{Fq}, m^*)(\nabla \rho_q)^2 + B_{2q}(k_{Fq}, m^*)(\nabla \rho_q \cdot \nabla m^*) \\ + B_{3q}(k_{Fq}, m^*)(\nabla m^*)^2]. \quad (5.7)$$

The subscript q denotes the charge state of each nucleon, $\rho = \rho_p + \rho_n$ is the total density, $k_{Fq} = (3\pi^2 \rho_q)^{1/3}$, and the functions B_{iq} are directly obtained from Eq. (3.23).

The semiclassical ground-state densities and the meson and photon fields are obtained by solving the Euler-Lagrange equations associated with the semiclassical energy density (5.5),

$$\varepsilon_{Fq} - m + g_v V_0 + e A_0 - 2B_{1q} \Delta \rho_q - B_{2q} \Delta m^* - \frac{\partial B_{1q}}{\partial \rho_q} (\nabla \rho_q)^2 - 2 \frac{\partial B_{1q}}{\partial m^*} (\nabla \rho_q \cdot \nabla m^*) \\ - \left(\frac{\partial B_{2q}}{\partial m^*} - \frac{\partial B_{3q}}{\partial \rho_q} \right) (\nabla m^*)^2 - \lambda_q = 0, \quad (5.8)$$

$$\Delta A_0 = -e \rho_p, \quad (5.9)$$

$$(\Delta - m_v^2) V_0 = -g_v \rho, \quad (5.10)$$

$$(\Delta - m_s^2) \phi_0 = -g_s \rho_s + b \phi_0^2 + c \phi_0^3, \quad (5.11)$$

where the semiclassical scalar density is

$$\begin{aligned} \rho_s = \frac{\partial e_0}{\partial m^*} - \sum_q \left[B_{2q} \Delta \rho_q + 2B_{3q} \Delta m^* + \left(\frac{\partial B_{2q}}{\partial \rho_q} - \frac{\partial B_{1q}}{\partial m^*} \right) (\nabla \rho_q)^2 \right. \\ \left. + 2 \frac{\partial B_{3q}}{\partial \rho_q} (\nabla \rho_q \cdot \nabla m^*) + \frac{\partial B_{3q}}{\partial m^*} (\nabla m^*)^2 \right]. \end{aligned} \quad (5.12)$$

The explicit evaluation of ρ_s from (5.12) leads to the expression already given in (3.22).

Unlike the case of external potentials, the scalar field ϕ_0 (and the effective mass m^*) is here self-consistently determined and receives explicitly a contribution of order \hbar^2 through ρ_s in Eq. (5.11). Therefore, one might think that m^* appearing in e_0 should be replaced by its expansion in a pure zero-order term m_0^* and a correction of order \hbar^2 , $\delta m^* = m^* - m_0^* + \mathcal{O}(\hbar^4)$, as discussed in Ref. [45]. If one wants to follow this route, one should proceed in a similar way as the one used in Section 3.2 to obtain the correction δk to the local Fermi momentum. Expanding the scalar density about k_0 and m_0^* ,

$$\begin{aligned} \rho_s(k_F, m^*) = \rho_{s,0}(k_0, m_0^*) + \left(\frac{\partial \rho_{s,0}(k_0, m_0^*)}{\partial k_0} \right) \delta k + \left(\frac{\partial \rho_{s,0}(k_0, m_0^*)}{\partial m_0^*} \right) \delta m^* \\ + \rho_{s,2}(k_0, m_0^*) + \mathcal{O}(\hbar^4), \end{aligned} \quad (5.13)$$

and imposing the condition

$$\rho_{s,0}(k_0, m_0^*) = \rho_s(k_F, m^*), \quad (5.14)$$

Equation (5.13) leads to

$$\delta m^* = - \left[\rho_{s,2}(k_0, m_0^*) - \frac{m_0^*}{\varepsilon_0} \rho_2(k_0, m_0^*) \right] \left(\frac{\partial \rho_{s,0}(k_0, m_0^*)}{\partial m_0^*} \right)^{-1}, \quad (5.15)$$

finally replacing k_0 by k_F (the subscript q is dropped to ease notation). Then, the semiclassical energy density (5.5) has an extra contribution:

$$e^{\text{sc}}(k_F, m^*) = e^{\text{sc}}(k_F, m_0^*) + \left(\frac{\partial e_0(k_F, m_0^*)}{\partial m_0^*} \right) \delta m^*. \quad (5.16)$$

The variational equations obtained from this new functional are formally the same as the set (5.8)–(5.11) if m^* is replaced by m_0^* and ρ_s by $\rho_{s,0}(k_F, m_0^*)$, except for Eq. (5.8), which has a new term on the l.h.s.,

$$\left(\frac{\partial \rho_s(k_F, m_0^*)}{\partial k_F} \right) \frac{\pi^2}{k_F^2} \delta m^*. \quad (5.17)$$

Proceeding in this manner, the following additional relation is obtained which provides the expression of m_0^* in terms of ϕ_0 :

$$m_0^* + \delta m^* = m^* = m - g_s \phi_0. \quad (5.18)$$

However, this decomposition of m^* is not essential to obtain the self-consistent densities, meson fields, and energies up to order \hbar^2 : the same Euler-Lagrange equations are obtained by expanding about m_0^* in the former set of equations (5.8)–(5.11) consistently to order \hbar^2 . Thus, the solutions of the original set of variational equations (5.8)–(5.11) implicitly contain the correction δm^* and, for all practical purposes, are the same as those which would be obtained starting from the functional (5.16). In addition, the technical problem of solving the variational equations simplifies if one does not have to go through Eq. (5.18) to obtain m_0^* at each iteration step.

5.1.2. Numerical Solution

This subsection is devoted to the numerical treatment of the second-order semiclassical variational equations. The field equations (5.9)–(5.11), together with the nucleon equation (5.8), constitute a set of coupled equations which ought to be solved simultaneously. The non-linear gradient terms in ρ and m^* make the numerical approach rather delicate. These difficulties notwithstanding, the task much resembles non-relativistic ETF calculations with Skyrme forces and similar iterative schemes can be employed.

To solve the nucleon equation (5.8) we rely on the so-called imaginary time step method [64, 65]. It is inspired from the way time-dependent HF equations are solved [66] and is currently used in static non-relativistic HF and ETF calculations. The time-dependent equation

$$i \frac{\partial}{\partial t} \varphi = \hat{h} \varphi \quad (5.19)$$

is formally solved as

$$\varphi(\Delta t) = \exp(-i \Delta t \hat{h}) \varphi(0). \quad (5.20)$$

If the time step Δt is replaced by an imaginary quantity $-i \Delta \tau$, the repeated action of the exponential

$$\varphi^{(n+1)} = \exp(-\Delta \tau \hat{h}) \varphi^{(n)}, \quad (5.21)$$

followed by a normalization of φ , causes the wave function to converge to the lowest eigenstate of \hat{h} [64].

In the semiclassical problem the Euler-Lagrange equation (5.8), $\delta e^{\text{sc}} / \delta \rho_q = \lambda_q$, is rewritten in the form

$$\left(-\frac{\xi}{2m} \Delta + W_q \right) \Phi_q = \lambda_q \Phi_q \quad (5.22)$$

by introducing $\Phi_q = \rho_q^{1/2}$ and

$$W_q = \frac{\delta e^{sc}}{\delta \rho_q} + \frac{\xi}{2m} \frac{\Delta \Phi_q}{\Phi_q}, \quad (5.23)$$

where ξ is an arbitrary constant. This is a Schrödinger-type eigenvalue equation for the ETF single-particle Hamiltonian $h_{\text{ETF}} = -\xi \Delta/(2m) + W_q$ which may be solved by application of the imaginary time step method [65].

The differential operators, densities, and fields are represented on a discrete mesh in coordinate space. In practice one works with a $[1, 1]$ Padé approximation to the exponential. The algorithm then reads

$$\left(1 + \frac{\Delta\tau}{2} h_{\text{ETF}}^{(n+1/2)}\right) \Phi_q^{(n+1)} = \left(1 - \frac{\Delta\tau}{2} h_{\text{ETF}}^{(n+1/2)}\right) \Phi_q^{(n)}, \quad (5.24)$$

where $h_{\text{ETF}}^{(n+1/2)}$ is calculated between steps n and $n+1$ (cf. Refs. [64, 66]). The Coulomb potential A_0 and the Yukawa potentials V_0 and ϕ_0 required at each iteration are evaluated by solving, respectively, the discrete Poisson and Helmholtz equations using Gaussian elimination [66].

The whole procedure can thus be described as follows:

- (i) Start from Fermi-shaped densities ρ_q and ρ_s .
- (ii) After the n th-iteration stage, the scalar meson potential $\phi_0^{(n+1)}$ is found by Gaussian elimination of the discrete radial equation

$$\left(\frac{d^2}{dr^2} - m_s^2\right) (r\phi_0^{(n'+1)}) = r\{-g_s\rho_s[\rho_q^{(n)}, \phi_0^{(n')}] + b(\phi_0^{(n')})^2 + c(\phi_0^{(n')})^3\}. \quad (5.25)$$

The new index n' indicates that, between steps n and $n+1$, Eq. (5.25) has to be iterated until consistency in $\phi_0^{(n+1)}$ is achieved. The presence of second-order derivatives of ϕ_0 in ρ_s can make this condition difficult to fulfil [41]. Note that in (5.25) the scalar density ρ_s is iterated without changing $\rho_q^{(n)}$. The boundary conditions imposed at the origin and at the infinite mesh point are $r\phi_0 = 0$. The results are quite similar if, instead of these boundary conditions, a vanishing slope of ϕ_0 is chosen at the mesh boundaries. The potentials $A_0^{(n+1)}$ and $V_0^{(n+1)}$ are generated by similar techniques (now only one elimination in Eqs. (5.9) and (5.10) is required).

(iii) With the new potentials compute $h_{\text{ETF}}^{(n+1/2)}$ and obtain $\Phi_q^{(n+1)}$ according to (5.24), with Φ_q subject to the boundary condition that $d\Phi_q/dr$ vanishes at the origin and at the mesh edge. Normalize $\rho_q^{(n+1)}$ to the particle number. Check numerical convergence.

The steps (ii) and (iii) are then repeated until the desired accuracy is attained. The calculations have been performed on a mesh with a spacing $\Delta r = 0.1$ fm. The r -derivatives have been discretized using seven-point formulae although, in practice, simpler formulae suffice. The parameters ξ and $\Delta\tau$ are not independent and criti-

cally influence the rate of convergence. Typical values are $\xi \sim 2 \times 10^5 \text{ MeV}^2 \cdot \text{fm}^2$ and $\Delta\tau \sim 2.5 \times 10^{-23} \text{ s}$. The code runs until the condition

$$\sum_i \frac{|\Phi^{(n+1)}(r_i) - \Phi^{(n)}(r_i)|}{\Phi^{(n+1)}(r_i)} \leq 10^{-6} \quad (5.26)$$

is satisfied (the total energy converges much faster than the densities).

In the imaginary time step method the chemical potential λ_q is issued as a by-product and can be used as an additional test of the degree of convergence achieved. It has been found that $\delta e^{\text{sc}}/\delta\rho_q$ is independent of the position to a few parts in 10^7 when it is computed from the converged densities. Alternatively, the chemical potential can be obtained from the total energy of neighbouring nuclei as $\lambda_q = \Delta E/\Delta N_q$. Both methods yield chemical potentials that agree to a value of less than 0.1%. These controls leave little room for numerical error.

5.1.3. Discussion of Results

The total energies (without including any centre-of-mass correction), proton and neutron rms radii corresponding to some spherical nuclei in the simple TF approximation (labelled $\text{TF}h^0$) and including h^2 corrections (labelled $\text{TF}h^2$) are shown in Tables III and IV for the parameter sets HII and HIV, respectively. The semiclassical results are compared with the quantal results calculated from the self-consistent Hartree approximation. From these tables it is seen that the $\text{TF}h^2$ approximation yields some overbinding in comparison with the Hartree approximation. The $\text{TF}h^0$ results lie between the Hartree and the $\text{TF}h^2$ ones for HII and below $\text{TF}h^2$ for HIV. As discussed in [41], the $\text{TF}h^0$ results show lower binding than the Hartree ones for parameter sets which have a small effective mass at saturation ($m^*/m \approx 0.55$), and show greater binding than $\text{TF}h^2$ for larger effective masses (HII has $m^*/m = 0.68$ and HIV has $m^*/m = 0.80$). The crossing point between $\text{TF}h^0$ and Hartree is around $m^*/m = 0.65$. This behaviour, which is also

TABLE III

Total Energies E (in MeV), Neutron rms Radii r_n (in fm) and Proton rms Radii r_p (in fm)
Obtained Using the Parameter Set HII

	Hartree			$\text{TF}h^2$			$\text{TF}h^0$		
	E	r_n	r_p	E	r_n	r_p	E	r_n	r_p
^{40}Ca	-325.9	3.10	3.17	-342.6	3.00	3.05	-332.0	3.06	3.11
^{48}Ca	-405.6	3.35	3.22	-430.6	3.25	3.16	-418.8	3.31	3.22
^{90}Zr	-752.4	4.03	4.00	-793.4	3.96	3.94	-774.1	4.01	4.00
^{116}Sn	-952.6	4.38	4.35	-1008.2	4.31	4.29	-985.5	4.36	4.34
^{140}Ce	-1160.3	4.66	4.61	-1203.9	4.60	4.57	-1178.7	4.65	4.61
^{208}Pb	-1629.4	5.31	5.24	-1696.5	5.27	5.23	-1664.7	5.31	5.27

Note. The listed energies have not been corrected for centre-of-mass motion.

TABLE IV
Same as Table III for the Parameter Set HIV

	Hartree			TFh^2			TFh^0		
	E	r_n	r_p	E	r_n	r_p	E	r_n	r_p
^{40}Ca	-392.3	3.20	3.27	-411.7	3.13	3.18	-428.3	3.14	3.19
^{48}Ca	-476.5	3.48	3.36	-511.0	3.38	3.32	-529.4	3.38	3.34
^{90}Zr	-868.6	4.21	4.18	-923.5	4.14	4.16	-950.7	4.15	4.17
^{116}Sn	-1099.3	4.56	4.58	-1169.3	4.52	4.53	-1201.2	4.53	4.55
^{140}Ce	-1334.0	4.87	4.87	-1394.4	4.83	4.84	-1430.2	4.84	4.85
^{208}Pb	-1869.9	5.56	5.55	-1970.7	5.54	5.56	-2016.9	5.55	5.58

found in non-relativistic calculations performed with Skyrme forces [41], is due to the effective mass and is not significantly affected by the value of the incompressibility of the parameterization. If we compare the Hartree with the TFh^0 and TFh^2 results, it can be seen that for the parameter set HII the agreement between TFh^0 and Hartree is better than between TFh^2 and Hartree. This agreement should be considered only as accidental, as semiclassical and quantal calculations do differ in the shell correction. Actually, the shell correction is not as well estimated in the TFh^0 approach as in the TFh^2 one because the semiclassical expansion in powers of \hbar is less converged in the former than in the latter.

Figure 3 shows the proton, neutron, and scalar densities of ^{208}Pb calculated in the Hartree, TFh^0 , and TFh^2 approximations using the parameterization HII. The semiclassical results do not present oscillations due to the absence of shell effects

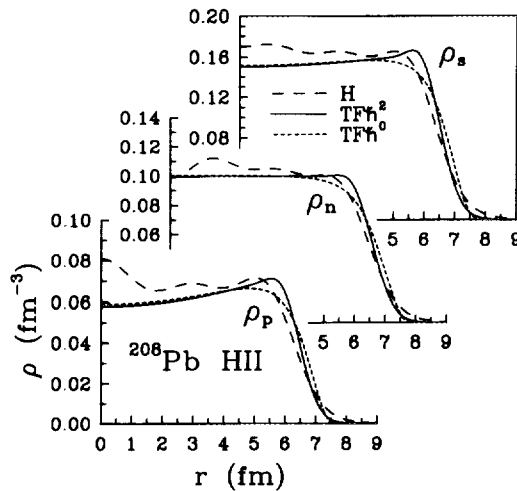


FIG. 3. Proton, neutron, and scalar densities of ^{208}Pb obtained with the parameterization HII in the Hartree (H), TFh^2 , and TFh^0 approximations.

but they average the Hartree densities. In the bulk the TFh^0 and TFh^2 densities are very similar. However, as expected, the gradient corrections incorporated by the TFh^2 functionals improve the densities at the surface, which come closer to the Hartree ones and show a better decay than the TFh^0 densities, despite the fact that the fall-off is still too steep in comparison with the Hartree solutions.

In Fig. 4 results obtained in lead with HII for the scalar meson potential $V_\sigma = g_s \phi_0$ and for the vector meson potential $V_\omega = g_v V_0$ are given. The radial dependence of the quantity

$$\alpha_{s.o.} = -\frac{1}{2m^2 r} \frac{d}{dr} (V_\sigma + V_\omega), \quad (5.27)$$

which is most sensitive to the nuclear surface, is also shown. A Foldy–Wouthuysen reduction of the Dirac equation for nucleons moving in the field generated by V_σ and V_ω relates $\alpha_{s.o.}$ with the strength of the non-relativistic single-particle effective spin–orbit force [2]. The TFh^2 calculation clearly overestimates the maximum value of $\alpha_{s.o.}$, but the position of the peak is closer to the Hartree result than with TFh^0 .

Finally, to sum up, there are two clear advantages the TFh^2 approximation has over the simple TFh^0 one. On the one hand, it provides fully variational densities that go exponentially to zero. On the other hand, it takes into account non-local spin–orbit and effective mass contributions up to order \hbar^2 , thus yielding a more reliable value of the semiclassically computed physical quantities.

5.2. Liquid Drop Model Coefficients

The surface energy in relativistic $\sigma - \omega$ models has been estimated by fitting a mass formula to finite nuclei results [34–36], or calculated from semi-infinite nuclear matter in the Hartree [7, 63] and TFh^0 [7, 37, 38] approximations. To our

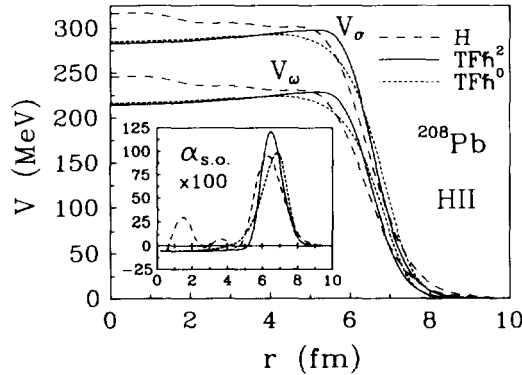


FIG. 4. Radial dependence of the scalar and vector meson potentials ($V_\sigma = g_s \phi_0$, $V_\omega = g_v V_0$) and of the quantity $\alpha_{s.o.}$, Eq. (5.27), calculated in ^{208}Pb with HII.

knowledge, no attempt has been made to calculate the curvature coefficient using a relativistic model.

In the liquid droplet model formulated by Myers and Swiatecki [24] the energy of a spherical nucleus is written as

$$E = a_v A + 4\pi \int_0^{\infty} dr r^2 [e(r) - a_v \rho(r)], \quad (5.28)$$

where a_v is the energy per particle in infinite nuclear matter and $e(r)$ and $\rho(r)$ are the energy and particle densities, respectively. Starting from (5.28) and following the method outlined in Refs. [24, 67], one obtains for the surface and curvature coefficients in semi-infinite nuclear matter the following expressions:

$$a_s = 4\pi r_0^2 \int_{-\infty}^{\infty} dz [e(z) - a_v \rho(z)]|_{\kappa=0}, \quad (5.29)$$

$$a_c = 8\pi r_0 \left[\int_{-\infty}^{\infty} dz (z - z_0) [e(z) - a_v \rho(z)]|_{\kappa=0} + \int_{-\infty}^{\infty} dz \frac{\partial [e(z) - a_v \rho(z)]}{\partial \kappa} \Big|_{\kappa=0} \right], \quad (5.30)$$

where $r_0 = [3/(4\pi\rho_0)]^{1/3}$ is the nuclear matter radius, z_0 is the location of the equivalent sharp surface, and κ is the curvature ($2/R$ for a sphere of radius R).

The two contributions to the curvature energy in (5.30) are called geometrical and dynamical, respectively. The geometrical contribution only involves the variation of the surface energy density $e(z) - a_v \rho(z)$ across the surface parallel to the z -axis, while the dynamical part corresponds to the variation of the surface energy density when the plane surface is infinitesimally bent. The surface energy density depends on the curvature κ in two different ways: one of them is the explicit

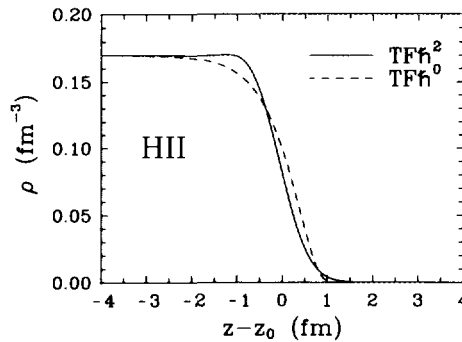


FIG. 5. Density profile of semi-infinite symmetric nuclear matter obtained with the parameter set HII in the TFh^2 and TFh^0 approximations.

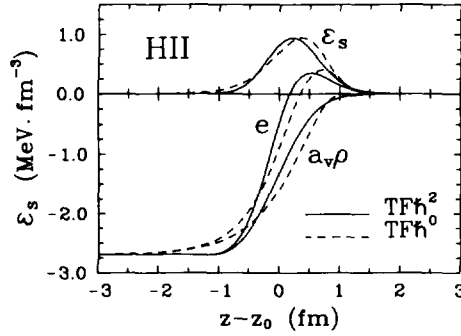


FIG. 6. Surface energy density $\mathcal{E}_s = e(z) - a_v\rho(z)$ calculated with the set HII. Also displayed is the separate contribution of the terms $e(z)$ and $a_v\rho(z)$.

dependence of $e(z)$ on the Δ operator (consider, for example, the non-relativistic definition of the kinetic energy density) which in the limit of $R \rightarrow \infty$ reads $d^2/dz^2 + \kappa d/dz$. The other one corresponds to the implicit curvature dependence of $\rho(z)$.

In the relativistic $\sigma - \omega$ model, the semiclassical energy density (5.5) is free of an explicit Δ dependence, since this dependence has been removed by partial integration. On the other hand, the implicit curvature dependence of the nuclear density ρ and of the meson fields V_0 and ϕ_0 does not contribute to the dynamical part of the curvature energy in a self-consistent calculation, because the surface tension of semi-infinite nuclear matter is stationary with respect to changes in the density and in the meson fields [24]. Consequently, the curvature energy is only given by its geometrical contribution.

Figure 5 displays the $\text{TF}\hbar^0$ and $\text{TF}\hbar^2$ density profiles of semi-infinite nuclear matter obtained with the set HII, and Figs. 6 and 7 show the $\text{TF}\hbar^0$ and $\text{TF}\hbar^2$ surface and curvature energy densities for HII. Table V collects the surface and curvature coefficients as well as the surface thickness of the semi-infinite density profile (standard 90% to 10% distance) calculated with the parameter sets PW1, P1, HII, and HIV. From this table it is seen that the quantal and semiclassical calculations

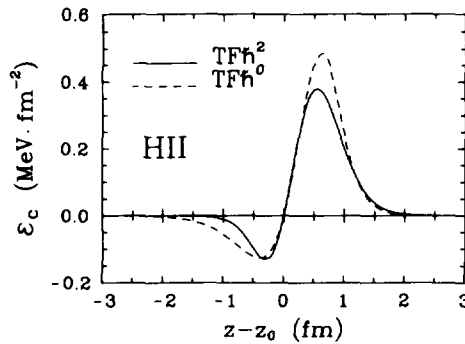


FIG. 7. Curvature energy density $\mathcal{E}_c = (z - z_0)[e(z) - a_v\rho(z)]$ calculated with the set HII.

TABLE V

Surface Energy (a_s), Surface Thickness (t), and Curvature Energy (a_c) Corresponding to Some Parameterizations of the $\sigma - \omega$ Model and to Different Thomas-Fermi Approximations

	m^*/m	κ (MeV)	a_s (MeV)			t (fm)			a_c (MeV)	
			H	TF \hbar^2	TF \hbar^0	H	TF \hbar^2	TF \hbar^0	TF \hbar^2	TF \hbar^0
PWI	0.56	546	33.8	32.8	35.9	2.38	2.27	2.71	18.8	20.1
P1	0.57	206	15.8	17.4	19.9	2.31	2.09	2.96	12.4	16.0
HI1	0.68	345		16.0	17.3		1.23	1.57	7.2	7.5
HI4	0.80	240		11.1	10.0		1.07	1.00	4.9	3.7

Note. Also displayed are some Hartree (H) results (from Ref. [63]) and the values of the effective mass and nuclear incompressibility κ at saturation.

of the surface coefficient and thickness agree fairly well. The values found for a_c are within the range of those obtained in semiclassical non-relativistic calculations using Skyrme forces [21, 68] (the empirical value is $a_c^{\text{emp}} \approx 0$ MeV [69]). The evolution as a function of the effective mass of the TF \hbar^0 results in comparison with the TF \hbar^2 ones shows the same trend as for finite nuclei.

As discussed by Hofer and Stocker [63], few parameterizations of the $\sigma - \omega$ model are able to simultaneously yield acceptable values for the surface energy and thickness (a_s should be around 16.5–21 MeV and t around 2.2–2.5 fm). Among the ones used here, only the parameterization P1 gives satisfactory results (see Table V).

6. SUMMARY

This paper has dealt with some technical aspects of semiclassical relativistic theory, which have been complemented with illustrative applications to finite nuclei and semi-infinite nuclear matter in the $\sigma - \omega$ model. A recurrent scheme to obtain the semiclassical \hbar expansion of the propagator associated with a time-independent single-particle Hamiltonian with a matrix structure has been given. In analogy to the non-relativistic case, the approach is based on the Wigner-Kirkwood expansion of the phase-space densities.

Attention has been focused on the application of the method to a Dirac Hamiltonian with a position-dependent effective mass, related to relativistic nuclear mean field theory. Compared with the non-relativistic case, the procedure is considerably more complicated owing to the matrix structure of the Hamiltonian. For this reason the \hbar series is only expanded to terms with \hbar^2 . The calculation of the Wigner-Kirkwood expressions of the density matrix and of the particle and energy densities, as well as the derivation of the corresponding density functional results, are thoroughly described. We hope that the self-contained presentation of the

methods developed here could be of some help in other studies on the formulation of semiclassical expansions.

The accuracy of the Wigner-Kirkwood series was tested on a relativistic harmonic oscillator and perfect agreement with the Strutinsky averaged observables was found even in the highly relativistic regime. The density functional version was shown to be slightly less accurate, a feature already known in the non-relativistic case. One can conclude from this model study that, for positive energy states, the derived semiclassical expansions contain all of the relativistic ingredients, the difference with quantal results being mainly due to shell effects.

Two of the most appealing advantages of a semiclassical formulation are physical transparency and the fact that certain observables are only accessible in a semiclassical framework. This is typical of the case of the curvature energy. Liquid drop model coefficients have been calculated for some parameter sets of the $\sigma - \omega$ model, and reasonable values for the surface thickness and for the surface and curvature energies have been found.

Finally, we would like to stress that well-behaved solutions of the semiclassical relativistic variational equations have been obtained. The existence of such solutions was not evident a priori. This means that further research into corrections of higher order in \hbar could prove to be a worthy and not merely an academic task.

APPENDIX A

It will be shown in this appendix that in the Wigner representation the Dirac Hamiltonian (2.10) is equal to its classical counterpart $H = \boldsymbol{\alpha} \cdot \mathbf{p} + \beta m^* + IV$. The Wigner transform of a single-particle operator $\hat{A}(x, x')$ in Minkowski space is defined by

$$A_w = A_w(q, p) = \int ds e^{ip \cdot s} \langle q + s/2 | \hat{A} | q - s/2 \rangle, \quad (\text{A.1})$$

where x and x' are four-vectors, p is the four-momentum, $q = (x + x')/2$, and $s = x - x'$. If \hat{A} is time-independent, (A.1) becomes

$$A_w = \int d\mathbf{s} e^{-i\mathbf{p} \cdot \mathbf{s}} \langle \mathbf{q} + \mathbf{s}/2 | \hat{A} | \mathbf{q} - \mathbf{s}/2 \rangle. \quad (\text{A.2})$$

Consider the case where \hat{A} is the Dirac Hamiltonian

$$\hat{H} = \hat{i} + \beta S + IV, \quad (\text{A.3})$$

with

$$\hat{i} = \boldsymbol{\alpha} \cdot \hat{\mathbf{p}} + \beta m. \quad (\text{A.4})$$

It is easy to see that $V_w = V(\mathbf{q})$ and $S_w = S(\mathbf{q})$, so that one only needs to calculate t_w .

The eigenstates of \hat{t} are the plane wave solutions of the free Dirac equation:

$$\hat{t} |\mathbf{p} \sigma e\rangle = e \tilde{\varepsilon} |\mathbf{p} \sigma e\rangle, \quad (\text{A.5})$$

where $\tilde{\varepsilon} = (p^2 + m^2)^{1/2}$, $\sigma = \pm 1/2$, and $e = \pm 1$. The 4×4 unit matrix can be expanded as

$$I = \sum_{\sigma, e} \int d\mathbf{p} |\mathbf{p} \sigma e\rangle \langle \mathbf{p} \sigma e|. \quad (\text{A.6})$$

Taking into account the fact that

$$\langle \mathbf{r} | \mathbf{p} \sigma e \rangle = u(\mathbf{p} \sigma e) \frac{e^{i\mathbf{p} \cdot \mathbf{r}}}{(2\pi)^{3/2}}, \quad (\text{A.7})$$

with

$$u(\mathbf{p} \sigma +) = \left(\frac{\tilde{\varepsilon} + m}{2\tilde{\varepsilon}} \right)^{1/2} \begin{pmatrix} 1 \\ \frac{\boldsymbol{\sigma} \cdot \mathbf{p}}{\tilde{\varepsilon} + m} \end{pmatrix} \chi_{\sigma} \quad (\text{A.8})$$

and

$$u(\mathbf{p} \sigma -) = \left(\frac{\tilde{\varepsilon} + m}{2\tilde{\varepsilon}} \right)^{1/2} \begin{pmatrix} -\frac{\boldsymbol{\sigma} \cdot \mathbf{p}}{\tilde{\varepsilon} + m} \\ 1 \end{pmatrix} \chi_{\sigma}, \quad (\text{A.9})$$

the Wigner transform of \hat{t} can be written as

$$\begin{aligned} t_w &= \sum_{\sigma, e} \int d\mathbf{p}' \int d\mathbf{s} e^{-i\mathbf{p}' \cdot \mathbf{s}} \langle \mathbf{q} + \mathbf{s}/2 | \hat{t} | \mathbf{p}' \sigma e \rangle \langle \mathbf{p}' \sigma e | \mathbf{q} - \mathbf{s}/2 \rangle \\ &= \sum_{\sigma, e} e \int d\mathbf{p}' \tilde{\varepsilon}' u(\mathbf{p}' \sigma e) u^\dagger(\mathbf{p}' \sigma e) \frac{1}{(2\pi)^3} \int d\mathbf{s} e^{i(\mathbf{p}' - \mathbf{p}) \cdot \mathbf{s}} \\ &= \tilde{\varepsilon} \sum_{\sigma, e} e u(\mathbf{p} \sigma e) u^\dagger(\mathbf{p} \sigma e). \end{aligned} \quad (\text{A.10})$$

Upon insertion of (A.8) and (A.9) into (A.10), a simple calculation leads to

$$t_w = \boldsymbol{\alpha} \cdot \mathbf{p} + \beta m \quad (\text{A.11})$$

and, hence,

$$H_w = \boldsymbol{\alpha} \cdot \mathbf{p} + \beta m^* + IV. \quad (\text{A.12})$$

APPENDIX B

The expression of the lowest term \mathcal{H}_0 in the semiclassical expansion of the density matrix for the Dirac Hamiltonian (2.10) has been given in Eq. (2.19). It has been shown to separately contain the positive and negative energy contributions. The \hbar -order term \mathcal{H}_1 and the \hbar^2 -order term \mathcal{H}_2 also have this property and can be written as

$$\mathcal{H}_1 = \mathcal{H}_1^+ + \mathcal{H}_1^-, \quad \mathcal{H}_2 = \mathcal{H}_2^+ + \mathcal{H}_2^-, \quad (\text{B.1})$$

The positive energy part of \mathcal{H}_1 is

$$\mathcal{H}_1^+ = \mathcal{H}_{1,I} + \mathcal{H}_{1,\beta} + \mathcal{H}_{1,\alpha} + \mathcal{H}_{1,\gamma}, \quad (\text{B.2})$$

with

$$\mathcal{H}_{1,I} = \frac{1}{4\epsilon^3} (\epsilon\delta + \Theta) \gamma^5 (\boldsymbol{\alpha} \cdot (\mathbf{p} \wedge \nabla V)), \quad (\text{B.3})$$

$$\mathcal{H}_{1,\beta} = \frac{1}{4\epsilon^3} (\epsilon\delta + \Theta) \gamma^5 (\boldsymbol{\gamma} \cdot (\mathbf{p} \wedge \nabla m^*)), \quad (\text{B.4})$$

$$\mathcal{H}_{1,\alpha} = 0, \quad (\text{B.5})$$

$$\mathcal{H}_{1,\gamma} = -\frac{i}{4\epsilon^3} [m^*(\epsilon\delta + \Theta)(\boldsymbol{\gamma} \cdot \nabla V) + \epsilon^2 \delta(\boldsymbol{\gamma} \cdot \nabla m^*)]. \quad (\text{B.6})$$

In the above equations the Dirac γ^5 and $\boldsymbol{\gamma}$ matrices [49] have been introduced. The argument of the Θ function and its derivatives is $\lambda^+ - V - \epsilon$. From Eqs. (B.3)–(B.6), it is seen that \mathcal{H}_1^+ has zero trace (when it is also taken over the spin degrees of freedom).

Using the same notation, the second-order term is

$$\mathcal{H}_2^+ = \mathcal{H}_{2,I} + \mathcal{H}_{2,\beta} + \mathcal{H}_{2,\alpha} + \mathcal{H}_{2,\gamma}, \quad (\text{B.7})$$

with

$$\begin{aligned} \mathcal{H}_{2,I} = & \frac{1}{48\epsilon^5} [(\epsilon^2\delta'' + 3\epsilon\delta' + 3\delta)[\epsilon^2(\nabla V)^2 - (\mathbf{p} \cdot \nabla V)^2 + m^{*2}(\nabla m^*)^2 \\ & + m^*(\mathbf{p} \cdot \nabla)^2 m^* + (\mathbf{p} \cdot \nabla m^*)^2] + (\epsilon^3\delta'' + 3\epsilon^2\delta' + 6\epsilon\delta + 6\Theta) \\ & \times [(\mathbf{p} \cdot \nabla)^2 V + 2m^*(\nabla V \cdot \nabla m^*)] - 3\epsilon^2(\epsilon^2\delta' + 2\epsilon\delta + 2\Theta) \Delta V \\ & - 3\epsilon^2 m^*(\epsilon\delta' + \delta) \Delta m^*] I, \end{aligned} \quad (\text{B.8})$$

$$\begin{aligned}
\mathcal{R}_{2,\beta} = & \frac{1}{48\varepsilon^7} [m^* \varepsilon^2 (\varepsilon^3 \delta'' - 3\varepsilon \delta - 3\Theta)(\nabla V)^2 - m^* (\varepsilon^3 \delta'' + 6\varepsilon^2 \delta' + 15\varepsilon \delta + 15\Theta) \\
& \times [(\mathbf{p} \cdot \nabla V)^2 - m^{*2} (\nabla m^*)^2 - m^* (\mathbf{p} \cdot \nabla)^2 m^* - (\mathbf{p} \cdot \nabla m^*)^2] \\
& - 3\varepsilon^2 (\varepsilon^2 \delta' + 3\varepsilon \delta + 3\Theta) [2m^* (\nabla m^*)^2 + (\mathbf{p} \cdot \nabla)^2 m^*] \\
& + m^* \varepsilon^2 (\varepsilon^2 \delta'' + 3\varepsilon \delta' + 3\delta) [(\mathbf{p} \cdot \nabla)^2 V + 2m^* (\nabla V \cdot \nabla m^*)] \\
& - 3\varepsilon^4 (\varepsilon \delta' + \delta) [2(\nabla V \cdot \nabla m^*) + m^* \Delta V] \\
& - 3\varepsilon^2 (m^{*2} \varepsilon^2 \delta' - 3p^2 \varepsilon \delta - 3p^2 \Theta) \Delta m^*] \beta,
\end{aligned} \tag{B.9}$$

$$\begin{aligned}
\mathcal{R}_{2,\alpha} = & \frac{1}{48\varepsilon^7} [\varepsilon^2 (\varepsilon^3 \delta'' - 3\varepsilon \delta - 3\Theta)(\nabla V)^2 - (\varepsilon^3 \delta'' + 6\varepsilon^2 \delta' + 15\varepsilon \delta + 15\Theta) \\
& \times [(\mathbf{p} \cdot \nabla V)^2 - m^{*2} (\nabla m^*)^2 - m^* (\mathbf{p} \cdot \nabla)^2 m^* - (\mathbf{p} \cdot \nabla m^*)^2] \\
& + \varepsilon^2 (\varepsilon^2 \delta'' + 3\varepsilon \delta' + 3\delta) [(\mathbf{p} \cdot \nabla)^2 V + 2m^* (\nabla V \cdot \nabla m^*)] \\
& - 3\varepsilon^4 (\varepsilon \delta' + \delta) \Delta V - 3m^* \varepsilon^2 (\varepsilon^2 \delta' + 3\varepsilon \delta + 3\Theta) \Delta m^*] (\boldsymbol{\alpha} \cdot \mathbf{p}) \\
& + \frac{1}{8\varepsilon^5} [(\varepsilon^2 \delta' + 3\varepsilon \delta + 3\Theta) \\
& \times [(\mathbf{p} \cdot \nabla V)(\boldsymbol{\alpha} \cdot \nabla V) - (\mathbf{p} \cdot \nabla m^*)(\boldsymbol{\alpha} \cdot \nabla m^*)]],
\end{aligned} \tag{B.10}$$

$$\mathcal{R}_{2,\gamma} = \frac{i}{8\varepsilon^5} (\varepsilon^2 \delta' + 3\varepsilon \delta + 3\Theta) (\mathbf{p} \cdot (\nabla V \wedge \nabla m^*)) \gamma^5 \beta. \tag{B.11}$$

The contributions of negative energy states are easily obtained from the positive terms by making the following substitution:

$$\begin{aligned}
\mathcal{R}_1(\varepsilon) &= \mathcal{R}_1^+(\varepsilon \rightarrow -\varepsilon, \lambda^+ \rightarrow \lambda^-), \\
\mathcal{R}_2(\varepsilon) &= \mathcal{R}_2^+(\varepsilon \rightarrow -\varepsilon, \lambda^+ \rightarrow \lambda^-).
\end{aligned} \tag{B.12}$$

APPENDIX C

As discussed in Section 2.3, the idempotency property (2.20) of the density matrix $\hat{\mathcal{R}}$ gives rise to relationships which the different orders of its semiclassical expansion have to satisfy, cf. Eq. (2.21). In the following it is shown that the well-known \hbar^2 -order Wigner–Kirkwood expansion of the density matrix $\hat{\rho}$ for a non-relativistic Hamiltonian

$$\hat{H} = \frac{\hat{p}^2}{2m} + V(\mathbf{r}) \tag{C.1}$$

fulfils

$$(\hat{\rho}^2)_w = (\hat{\rho})_w \equiv f \tag{C.2}$$

up to order \hbar^2 . This is a subtle proof since it involves the evaluation of products of distributions, and is useful for the relativistic generalization.

The Wigner transform of the Hamiltonian (C.1) is

$$H_w = \frac{p^2}{2m} + V \quad (C.3)$$

and the corresponding semiclassical density matrix reads [51]

$$f = f_0 + \hbar^2 f_2 \quad (C.4)$$

with

$$f_0 = \Theta(\lambda - H_w), \quad (C.5)$$

$$f_2 = -\frac{1}{8m} \Delta V \delta'(\lambda - H_w) + \frac{1}{24m} \left[(\nabla V)^2 + \frac{1}{m} (\mathbf{p} \cdot \nabla)^2 V \right] \delta''(\lambda - H_w). \quad (C.6)$$

At order \hbar^0 it is clear that $f_0^2 = f_0$. At second order, using Eq. (2.5):

$$\begin{aligned} (\hat{\rho}^2)_w &= (f_0 + \hbar^2 f_2) \left(1 + \frac{i\hbar}{2} \tilde{A} - \frac{\hbar^2}{8} \tilde{A}^2 \right) (f_0 + \hbar^2 f_2) \\ &= f_0^2 + \hbar^2 \left(2f_0 f_2 - \frac{1}{8} f_0 \tilde{A}^2 f_0 \right) \\ &= \Theta - \frac{\hbar^2}{4m} \left[\Delta V (\Theta \delta' + \delta^2) \right. \\ &\quad \left. - \left((\nabla V)^2 + \frac{1}{m} (\mathbf{p} \cdot \nabla)^2 V \right) \left(\frac{1}{3} \Theta \delta'' + \delta \delta' \right) \right]. \end{aligned} \quad (C.7)$$

To compare Eq. (C.7) with (C.6), it is necessary to interpret the products of the step function and its derivatives which appear in (C.7). For this purpose, let us recall two properties of distributions [70]:

$$\begin{aligned} \langle T^{(n)}, \varphi \rangle &= (-1)^n \langle T, \varphi^{(n)} \rangle, \\ \langle \phi T, \varphi \rangle &= \langle T, \phi \varphi \rangle, \end{aligned} \quad (C.8)$$

where T is a distribution (strictly speaking, a continuous linear functional on the space \mathcal{D} of the base functions [70]), $T^{(n)}$ is its n th-derivative, $\varphi \in \mathcal{D}$, and ϕ is a function of the class C_∞ . $\langle T, \varphi \rangle$ denotes the scalar which results from the action of T on φ . For example, $\langle \delta^{(n)}, \varphi \rangle = (-1)^n \varphi^{(n)}(0)$. From (C.8) it is easy to show that

$$\begin{aligned} \langle \Theta \delta, \varphi \rangle &= -\langle \Theta \delta, \varphi \rangle + \langle \delta, \varphi \rangle, \\ \langle \Theta \delta', \varphi \rangle &= -\langle \Theta \delta', \varphi \rangle - 2\langle \delta^2, \varphi \rangle + \langle \delta', \varphi \rangle, \\ \langle \Theta \delta'', \varphi \rangle &= -\langle \Theta \delta'', \varphi \rangle - 6\langle \delta \delta', \varphi \rangle + \langle \delta'', \varphi \rangle. \end{aligned} \quad (C.9)$$

And, formally, the following equations are obtained:

$$\begin{aligned}\Theta\delta &= \frac{1}{2}\delta, \\ \Theta\delta' + \delta^2 &= \frac{1}{2}\delta', \\ \frac{1}{3}\Theta\delta'' + \delta\delta' &= \frac{1}{6}\delta''.\end{aligned}\tag{C.10}$$

Inserting (C.10) into (C.7), (C.2) is proven to order \hbar^2 (we mention that a more indirect proof has been given in Ref. [16, p. 191]). The verification that the relativistic density matrix given in Appendix B fulfils Eq. (2.21) follows along the same lines, and only the relations (C.10) are required.

ACKNOWLEDGMENTS

We are very grateful to Saturnino Marcos for supplying us with the Hartree results used in Section 5.1, to Michel Farine for an interesting discussion about the content of Section 5.2, and to Detlef Von-Eiff and Professor Manfred K. Weigel for valuable comments. We are indebted to Martí Pi whose expertise allowed the development of the computer codes needed to obtain the semiclassical results presented in Section 5. This work has been supported in part by the IN2P3-CICYT exchange program and by the DGICYT (Spain) Grant PB89-0332.

REFERENCES

1. J. D. WALECKA, *Ann. Phys. (N.Y.)* **83** (1974), 491; S. A. CHIN AND J. D. WALECKA, *Phys. Lett. B* **52** (1974), 24.
2. B. D. SEROT AND J. D. WALECKA, *Adv. Nucl. Phys.* **16** (1986), 1.
3. P.-G. REINHARD, *Rep. Prog. Phys.* **52** (1989), 439.
4. C. J. HOROWITZ AND B. D. SEROT, *Nucl. Phys. A* **368** (1981), 503.
5. P.-G. REINHARD, M. RUF, J. MARUHN, W. GREINER, AND J. FRIEDRICH, *Z. Phys. A* **323** (1986), 13.
6. Y. K. GAMBHIR, P. RING, AND A. THIMET, *Ann. Phys. (N.Y.)* **198** (1990), 132.
7. J. BOGUTA AND A. R. BODMER, *Nucl. Phys. A* **292** (1977), 413.
8. J. BOGUTA AND H. STÖCKER, *Phys. Lett. B* **120** (1983), 289.
9. J. BOGUTA AND S. A. MOSZKOWSKI, *Nucl. Phys. A* **403** (1983), 445.
10. A. BOUYSSY, S. MARCOS, AND PHAM VAN THIEU, *Nucl. Phys. A* **422** (1984), 541.
11. A. BOUYSSY, J.-F. MATHIOT, NGUYEN VAN GIAI, AND S. MARCOS, *Phys. Rev. C* **36** (1987), 380.
12. P. G. BLUNDEN AND M. J. IQBAL, *Phys. Lett. B* **196** (1987), 295.
13. L. S. CELENZA AND C. M. SHAKIN, "Relativistic Nuclear Physics: Theories of Structure and Scattering," World Scientific, Singapore, 1986.
14. B. TER HAAR AND R. MALFLET, *Phys. Rep.* **149** (1987), 207.
15. R. BROCKMANN AND R. MACHLEIDT, *Phys. Rev. C* **42** (1990), 1965; H. MÜTHER, R. MACHLEIDT, AND R. BROCKMANN, *Phys. Rev. C* **42** (1990), 1981.
16. R. W. HASSE, R. ARVIEU, AND P. SCHUCK (Eds.), "Workshop on Semiclassical Methods in Nuclear Physics," *J. Phys. Colloq. C* **6** (1984).
17. R. M. DREIZLER AND J. DA PROVIDENCIA (Eds.), "Density Functional Methods in Physics," Vol. 123, NATO ASI Ser. B, Plenum, New York, 1985.
18. R. ARVIEU, M. DURAND, P. SCHUCK, AND E. SURAUD (Eds.), "International Workshop on Semiclassical and Phase Space Approaches to the Dynamics of the Nucleus," *J. Phys. Colloq. C* **2** (1987).
19. E. WIGNER, *Phys. Rev.* **40** (1932), 749; J. G. KIRKWOOD, *Phys. Rev.* **44** (1933), 31; G. E. UHLENBECK AND E. BETH, *Physica* **3** (1936), 729.

20. O. BOHIGAS, X. CAMPI, H. KRIVINE, AND J. TREINER, *Phys. Lett. B* **64** (1976), 381.
21. M. BRACK, C. GUET, AND H.-B. HÅKANSSON, *Phys. Rep.* **123** (1985), 275.
22. K. A. BRUECKNER, J. R. BUCHLER, S. JORNA, AND R. J. LOMBARD, *Phys. Rev.* **171** (1968), 1188.
23. P. HOHENBERG AND W. KOHN, *Phys. Rev.* **136** (1964), B864.
24. W. D. MYERS AND W. J. SWIATECKI, *Ann. Phys. (N.Y.)* **55** (1969), 395; **84** (1974), 186.
25. V. M. STRUTINSKY, *Nucl. Phys. A* **95** (1967), 420; **122** (1968), 1.
26. M. CENTELLES, M. PI, X. VIÑAS, F. GARCÍAS, AND M. BARRANCO, *Nucl. Phys. A* **510** (1990), 397.
27. M. V. RAMANA AND A. K. RAJAGOPAL, *Adv. Chem. Phys.* **54** (1983), 231.
28. D. A. KIRZHITS, "Field Theoretical Methods in Many-Body Systems," Pergamon, Oxford, 1967.
29. P. MALZACHER AND R. M. DREIZLER, *Z. Phys. D* **2** (1986), 37.
30. E. ENGEL AND R. M. DREIZLER, *Phys. Rev. A* **35** (1987), 3607.
31. E. ENGEL, H. MÜLLER, AND R. M. DREIZLER, *Phys. Rev. A* **39** (1989), 4873.
32. H. MÜLLER, E. ENGEL, AND R. M. DREIZLER, *Phys. Rev. A* **40** (1989), 5542.
33. W. F. POHLNER AND R. M. DREIZLER, *Phys. Rev. A* **44** (1991), 7165.
34. J. BOGUTA AND J. RAFELSKI, *Phys. Lett. B* **71** (1977), 22.
35. F. E. SERR AND J. D. WALECKA, *Phys. Lett. B* **79** (1978), 10.
36. B. D. SEROT AND J. D. WALECKA, *Phys. Lett. B* **87** (1979), 172.
37. W. STOCKER AND M. M. SHARMA, *Z. Phys. A* **339** (1991), 147.
38. M. M. SHARMA AND P. RING, ISN Grenoble Preprint 91.08, 1991.
39. M. CENTELLES, X. VIÑAS, M. BARRANCO, AND P. SCHUCK, *Nucl. Phys. A* **519** (1990), 73c.
40. K. TARUSHI AND P. SCHUCK, *Z. Phys. A* **342** (1992), 397.
41. M. CENTELLES, X. VIÑAS, M. BARRANCO, S. MARCOS, AND R. J. LOMBARD, *Nucl. Phys. A* **537** (1992), 486.
42. M. CENTELLES, X. VIÑAS, M. BARRANCO, N. OHTSUKA, A. FAESSLER, DAO TIEN KHOA, AND H. MÜTHER, *J. Phys. G* **17** (1991), L193; Barcelona University Preprint, 1992.
43. M. K. WEIGEL, S. HADDAD, AND F. WEBER, *J. Phys. G* **17** (1991), 619.
44. D. VON-EIFF AND M. K. WEIGEL, *Z. Phys. A* **339** (1991), 63.
45. C. SPEICHER, R. M. DREIZLER, AND E. ENGEL, *Ann. Phys. (N.Y.)* **213** (1992), 312.
46. P. RING AND P. SCHUCK, "The Nuclear Many-Body Problem," Chap. 13, Springer-Verlag, New York, 1980.
47. R. K. BHADURI AND C. K. ROSS, *Phys. Rev. Lett.* **27** (1971), 606; B. K. JENNINGS AND R. K. BHADURI, *Nucl. Phys. A* **237** (1975), 149; B. K. JENNINGS, R. K. BHADURI, AND M. BRACK, *Nucl. Phys. A* **253** (1975), 29.
48. B. GRAMMATICOS AND A. VOROS, *Ann. Phys. (N.Y.)* **123** (1979), 359; **129** (1980), 153.
49. J. D. BJORKEN AND S. D. DRELL, "Relativistic Quantum Mechanics," McGraw-Hill, New York, 1964.
50. M. ABRAMOWITZ AND I. A. STEGUN, "Handbook of Mathematical Functions," Dover, New York, 1965.
51. B. K. JENNINGS, *Phys. Lett. B* **74** (1978), 13.
52. D. VON-EIFF, S. HADDAD, AND M. K. WEIGEL, *Phys. Rev. C* **46** (1992), 230.
53. J. BARTEL, M. BRACK, AND M. DURAND, *Nucl. Phys. A* **445** (1985), 263.
54. G. B. SMITH AND L. J. TASSIE, *Ann. Phys. (N.Y.)* **65** (1971), 352.
55. R. TEGEN, *Ann. Phys. (N.Y.)* **197** (1990), 439.
56. V. I. KUKULIN, G. LOYOLA, AND M. MOSHINSKY, *Phys. Lett. A* **158** (1991), 19.
57. M. BRACK AND H. C. PAULI, *Nucl. Phys. A* **207** (1973), 401.
58. B. K. JENNINGS, *Nucl. Phys. A* **207** (1973), 538.
59. M. PRAKASH, S. SHLOMO, AND V. M. KOLOMIETZ, *Nucl. Phys. A* **370** (1981), 30.
60. J. RAMSCHÜTZ, F. WEBER, AND M. K. WEIGEL, *J. Phys. G* **16** (1990), 987.
61. J. BOGUTA, *Phys. Lett. B* **109** (1982), 251.
62. N. K. GLENDENNING, *Phys. Lett. B* **185** (1987), 275.
63. D. HOFER AND W. STOCKER, *Nucl. Phys. A* **492** (1989), 637.
64. K. T. R. DAVIES, H. FLOCARD, S. KRIEGER, AND M. S. WEISS, *Nucl. Phys. A* **342** (1980), 111.

65. S. LEVIT, *Phys. Lett. B* **139** (1984), 147; D. DALILI, J. NÉMETH, AND C. NGÔ, *Z. Phys. A* **321** (1985), 335.
66. P. BONCHE, S. KOONIN, AND J. W. NEGELE, *Phys. Rev. C* **13** (1976), 1226; K. T. R. DAVIES AND S. E. KOONIN, *Phys. Rev. C* **23** (1981), 2042.
67. W. STOCKER AND M. FARINE, *Ann. Phys. (N.Y.)* **159** (1985), 255.
68. W. STOCKER, J. BARTEL, J. R. NIX, AND A. J. SIERK, *Nucl. Phys. A* **489** (1988), 252.
69. P. MÖLLER, W. D. MYERS, W. J. SWIATECKI, AND J. TREINER, *At. Data Nucl. Data Tables* **39** (1988), 225.
70. R. GOUYON, "Intégration et Distributions," p. 71 ff, Vuibert, Paris, 1967.